Technologies and Processes for the Advancement of Materials

Thermal processing

ISSUE FOCUS ///

CRYOGENICS / VACUUM HEATING

EFFECT OF HEAT AND CRYOGENIC TREATMENT ON WEAR AND TOUGHNESS OF HSS AISI M2

COMPANY PROFILE ///

Buehler

JANUARY 2022
thermalprocessing.com

aichelin group

AFC HOLCROFT

industrial furnace solutions

Batch Integral Quench Furnaces and Endothermic Gas Generators "Built for Stock"

Leading the Industry with the Fastest Delivery Available

AFC-Holcroft Headquarters
Wixom, Michigan, USA
Phone: +1 248 624 8191

AFC-Holcroft Europe
Swiebodzin, Poland
Phone: +48 68 41 61 776

AFC-Holcroft Asia
Shanghai, P. R. China
Phone +86 21 5899 9100

www.afc-holcroft.com

Supply chain interruptions don't have to derail your valuable heat treating production. When you need a new batch integral quench furnace or endothermic gas generator, AFC-Holcroft's Built for Stock equipment will shave months off typical delivery timeframes.

We're always building our industry-leading UBQ (Universal Batch Quench) furnaces and EZ™ Series Endo Gas Generators for off-the-shelf delivery, ready for expedited shipment. The same standard equipment AFC-Holcroft is known for, but pre-built to speed up typical delivery by months. There is no compromise in quality to get this fast delivery.

Built for Stock equipment gets you in production faster.

Talk to our Sales staff to find out more.

GASBARRE
THERMAL PROCESSING SYSTEMS

RELIABILITY, EXPERTISE, SERVICE AND SELECTION

VERSATILE ***INTEGRAL QUENCH FURNACES***

- **Batch processing**
- **Compatible with existing equipment lines**
- **Highly efficient**
- **Precise control**
- **Meets AMS 2750 and CQI-9 Requirements**

Gasbarre takes a ***360° approach*** to ***servicing our customers***. From sales and applications engineering, to equipment design, manufacturing, commissioning, and never ending aftermarket support our team of engineers, metallurgists, and technicians ***understand your process*** from all angles. Gasbarre's technical capability and commitment to service will ***ensure your success*** today and into the future!

COMPLETE LINE OF THERMAL PROCESSING EQUIPMENT

Annealing ▪ Brazing ▪ Carbonitriding ▪ Carburizing ▪ Co-firing ▪ Drying ▪ Enameling
Ferritic Nitrocarburizing ▪ Glass-to-Metal Sealing ▪ Hardening ▪ Inert Atmosphere Processing
Nitriding ▪ Normalizing ▪ Quenching ▪ Sintering ▪ Soldering ▪ Spheroidize Annealing
Steam Treating ▪ Stress Relieving ▪ Tempering ▪ Vacuum Processes

734.656.2000
GasbarreIFS@gasbarre.com
www.gasbarre.com

GASBARRE
THERMAL PROCESSING SYSTEMS

CONTENTS ///

COVER PHOTO: SHUTTERSTOCK (3) / ILLUSTRATION BY RICK FRENNEA

WISCONSIN OVEN

SDB SERIES BATCH DRAW OVEN

40 Standard Models • Electric or Gas Heat

The Ultimate Draw Batch Oven:

- **Standard sizes** to match most heat treat lines
- **Temperatures to 1,400° F**
- **High capacity recirculation blower** for outstanding uniformity and heating rates
- **Available hearths include pier, skid, roller rails, & full width rollers**
- **Chain guides, charge cars and quench tanks also available**
- **Available with our exclusive Energy Efficient E-Pack™ oven upgrade** (see www.oven-epack.com for further info)
- **Built to Last!** Backed by our Exclusive and Unprecedented 3-Year WOW™ warranty
- **Additional sizes and features** available upon request

data sense technologies

Available with DataSense Technologies™ IoT Based Performance Monitoring System

WISOVEN.COM

sales@wisoven.com
262-642-3938

Wisconsin Oven Corporation
2675 Main Street • PO Box 873 East Troy, WI 53120

TPS Thermal Product Solutions

Wisconsin Oven is a brand of Thermal Product Solutions, LLC

DEPARTMENTS ///

JANUARY 2022 VOLUME 11 / NUMBER 1

UPDATE ///

New Products, Trends, Services & Developments

Q&A ///

PETER CAINE

DIRECTOR OF CUSTOM PRODUCTS ///
HEATTEK

RESOURCES ///

International Federation for Heat Treatment (IFHTSE)

The international association whose primary interest is heat treatment and surface engineering shares news of its activities to promote collaboration on issues affecting the industry. **12**

Industrial Heating Equipment Association (IHEA)

The national trade association representing the major segments of the industrial heat processing equipment industry shares news of it's activities, training, and key developments in the industry. **14**

HOT SEAT ///

The compatibility of different metallic and non-metallic materials with polymer quenchants is generally good. However, specific combinations should be tested before application. **16**

QUALITY COUNTS ///

Motivation comes from several directions, and transforming work into mini challenges presents workers a chance to use their skills to achieve success and feel invested. **18**

Thermal Processing is published monthly by Media Solutions, Inc., 266D Yeager Parkway Pelham, AL 35124. Phone (205) 380-1573 Fax (205) 380-1580 International subscription rates: $105.00 per year. Postage Paid at Pelham AL and at additional mailing offices. Printed in the USA. POSTMASTER: Send address changes to *Thermal Processing* magazine, P.O. Box 1210 Pelham AL 35124. Return undeliverable Canadian addresses to P.O. Box 503 RPO West Beaver Creek Richmond Hill, ON L4B4R6.

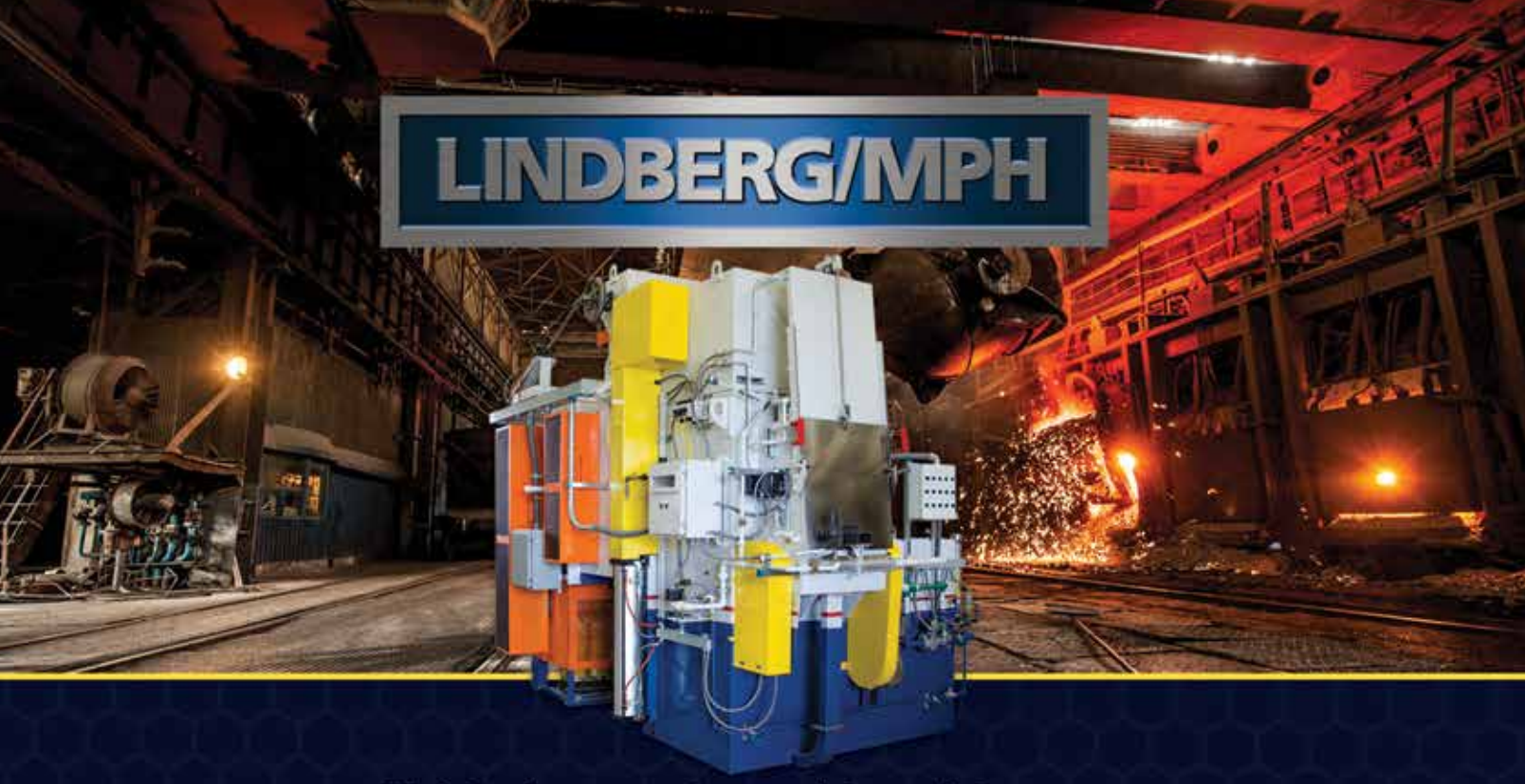

High Performance Integral Quench Systems

The Lindberg/MPH Integral Quench Furnace System is highly productive and efficient. It is available as either gas-fired or electrically heated and features obstruction-free chambers and strategically located heated sources to ensure rapid heat transfer, low energy use, and excellent temperature and carbon uniformity. As a leading OEM supplier our aftermarket team is trained to provide parts and service support on any industrial furnace or oven regardless of manufacturer.

Equipment Features

- Excellent uniformity for consistent processing
- Highly productive & efficient for quick, quality results
- Environmentally friendly with low energy use
- Chamber size and load movement configurations to suit your exact needs
- Fully automatic load movement
- Programmable logic controller

Companion Equipment

Pacemaker® Companion Washer | Pacecar | Pacemaker® Companion Draw Furnace

www.lindbergmph.com • Email: lindbergmph@lindbergmph.com • Phone: (269) 849-2700 • Fax: (269) 849-3021

TPS | Lindberg/MPH is a brand of Thermal Product Solutions, LLC.

FROM THE EDITOR ///

Another challenging year behind us

Happy New Year to all our readers in the heat-treat world, and, although New Year's Day wasn't a reset button, it did serve as a turning point into what we all hope will be a brighter future in 2022.

To get you primed for the new year, our first issue takes a look at cryogenics and vacuum heating. For those topics, we're bringing you some highly technical articles.

On the subject of cryogenics, our cover article looks at the effect of heat and cryogenic treatment on the wear and toughness of HSS AISI M2 and how cryogenic treatment should not be considered as only an add-on process.

Vacuum heating has been an essential part of the heat-treating industry for years, and it's an important process especially for treating aluminum and aluminum alloys. Our second January article investigates the effect of vacuum heat treatment on microstructures and the mechanical properties of 7A52 aluminum alloy-Al_2O_3 ceramic brazed joints.

Our third article, although not part of our January focus, still offers some vital expertise. The article, from Scot E. Coble, Jacob P. Feldbauer, Amber Tims, Craig Stringer, and Stephen L. Feldbauer, looks at the impact of complete lubricant removal on the mechanical properties and production of powder-metal components.

And make sure you check out what our columnists have cooked up for January as well. They are always sharing some fascinating information.

I hope you enjoy these articles and much more as we enter the new year and continue to share the good news and fascinating stories of the heat-treat industry.

And since it is the first of the year, I will take this opportunity to remind all of you that I am always on the lookout for articles and other submissions. It's a great way to share your expertise while shining a spotlight on you and your company at the same time. Hit me up if you have an article idea.

Take stock in the fact that we chugged through a challenging 2021 on the heels of its more twisted sister, 2020. So, join me and my team as we look to make 2022 even better. And let's all cross our fingers that 2022 doesn't also mean 2020 ... *too*.

Happy New Year, and, as always, thanks for reading!

KENNETH CARTER, EDITOR
editor@thermalprocessing.com
(800) 366-2185 x204

CALL FOR ARTICLES Have a technical paper or other work with an educational angle? Let Thermal Processing publish it. Contact the editor, Kenneth Carter, at *editor@thermalprocessing.com* for how you can share your expertise with our readers.

Thermal processing

David C. Cooper
PUBLISHER

EDITORIAL
Kenneth Carter
EDITOR
Jennifer Jacobson
ASSOCIATE EDITOR
Joe Crowe
ASSOCIATE EDITOR | SOCIAL MEDIA

SALES
Dave Gomez
NATIONAL SALES MANAGER
Ben Keaten
REGIONAL SALES MANAGER

CIRCULATION
Teresa Cooper
MANAGER
Jamie Willett
ASSISTANT

DESIGN
Rick Frennea
CREATIVE DIRECTOR
Michele Hall
GRAPHIC DESIGNER

CONTRIBUTING WRITERS
SCOT E. COBLE
DIEISON G.FANTINELI
JACOB P. FELDBAUER
STEPHEN L. FELDBAUER
D. SCOTT MACKENZIE
CLEBER T.PARCIANELLO
AFONSO REGULY
TONILSON S.ROSENDO
CRAIG STRINGER
TONY TENAGLIER
MARCO D.TIER
AMBER TIMS

Media solutions

PUBLISHED BY MEDIA SOLUTIONS, INC.
P. O. BOX 1987 • PELHAM, AL 35124
(800) 366-2185 • (205) 380-1580 FAX

David C. Cooper
PRESIDENT
Teresa Cooper
OPERATIONS

RTD vs. Thermocouple

RTD and thermocouples have important roles in temperature monitoring. Check out the chart below to determine which probe is best for your application!

	THERMOCOUPLE	RTD
Temperature	Measure temperatures -270 °C to +2300 °C	Measure temperatures -200 °C to +850 °C
Accuracy	Typical accuracy of up to 1 °C with a wider temperature range	An accuracy of 0.1 °C and repeatable results with a smaller temperature range
Sensitivity	Fast response time to change in temperature, about 3x faster than RTDs	Some are able to compete with thermocouples, but in general, are slower
Stability	Over time, readings can drift due to oxidation to the sensor, etc.	Better for long time use as they remain stable and offer repeatable measurements
Cost	Often less expensive and budget friendly for multi-probe applications	The accuracy of RTDs comes at a cost, running up to 3x higher than thermocouples

MadgeTech's brand new X-Series monitors up to 16 channels with just one device and features both thermocouple and RTD options to best fit your needs.

TCTempX

- Measures Temperatures up to 1820 °C (Probe Dependent)
- Supports a Variety of Thermocouples
- Individual Cold Junction Compensation

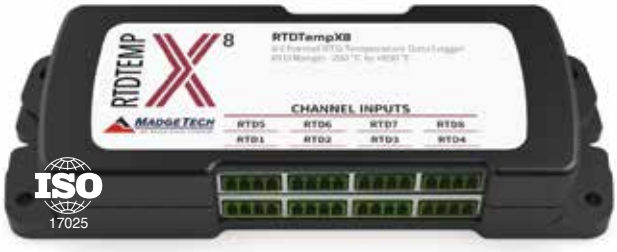

RTDTempX

- Accepts 2, 3 and 4-Wire RTDs
- Memory Capacity of 2,700,000+ Readings
- Measures Temperatures from -200 °C to +850 °C

MadgeTech data loggers are designed, manufactured and serviced in the USA and distributed worldwide.

MADGETECH
WE BUILD DATA LOGGERS

(603) 456-2011
madgetech.com

6 Warner Road
Warner, NH 03303

Solar Atmospheres of California's new small vacuum furnace was specifically designed to process a variety of materials between 600°F – 2,400°F (+/-10°F) in both vacuum and/or partial pressure environments. (Courtesy: Solar Atmospheres)

Solar Atmospheres of California adds small furnace capacity

To support R&D and additive manufacturing projects, Solar Atmospheres of California (SCA) has added some much-needed small vacuum furnace capacity to its expansive equipment offerings. The new vacuum furnace was procured from SCA's furnace manufacturing sister facility, Solar Manufacturing (SAMI), located in Sellersville, Pennsylvania, and was specifically designed to process a variety of materials between 600°F – 2,400°F (+/-10°F) in both vacuum and/or partial pressure environments. Precise cooling capability up to 2 bar in argon, nitrogen, or helium is available with a maximum operating temperature up to 2,650°F. The furnace is also equipped with the SAMI's state-of-the-art SolarVac® Polaris Control System for optimum performance and precise cycle control.

SCA president Derek Dennis said, "We are pleased to add this needed piece of vacuum furnace equipment to service our valuable customers. The additive manufacturing industry continues to grow, and this new furnace will allow SCA to respond to small builds and R&D projects quickly and precisely. SCA has become the go-to source for additive heat treating on the West Coast and we want to make sure we are making the necessary investments to support our customers' immediate needs and requirements. SCA will continue to focus on the best quality and on-time delivery with a focus on providing the best customer service in the industry. SCA has plans to add additional equipment in the future to ensure that we have the capacity available to handle the rebounding industry post-COVID."

MORE INFO www.solaratm.com

InfoSight founder John A. Robertson dies at 80

Dr. John A. Robertson, founder, chairman, CEO, and heart and soul of InfoSight Corporation in Chillicothe, Ohio, died December 2, 2021.

He was the epitome of the innovator, constantly searching for and creating unique ways to make the world a better place. His creativity was boundless and his honors include holding 56 patents, being president of the Electrostatic Society of America, a Fellow in the Instrument Society of America, named to the AIDC100 Hall of Fame, a graduate of the Harvard Business School OPM Program, and recognized as Entrepreneur of the Year twice. He was especially proud of Barbara, his wife of 46 years, his children, grandchildren, and great-grandchildren.

Dr. John A. Robertson, 1941-2021.

Robertson grew up in Blue Island, Illinois, and was chosen as one of 39 students to learn "new math." After graduation he attended DeVry Institute and earned a degree in electronics. Robertson worked in a number of jobs including repairing TVs, fixing Heath Kit projects after their owners had given up, as a station engineer for a broadcast station in Chicago, and as a technician at Fermi Labs.

Robertson later earned a Ph.D. in electrical engineering and physics from the University of Illinois, starting his classes at Navy Pier and finishing his research in Champagne.

Upon graduation in 1969, Robertson was recruited by Mead Corporation Central Research in Chillicothe. While at Mead he received his first ten patents and became recognized as a world expert in high-speed

SEND US YOUR NEWS Companies wishing to submit materials for inclusion in Thermal Processing's Update section should contact the editor, Kenneth Carter, at editor@thermalprocessing.com. Releases accompanied by color images will be given first consideration.

ink jet technology.

Robertson took an extended leave of absence to attempt sailing around the world in a 42-foot sloop that he rebuilt. He returned periodically to do some consulting but eventually accepted that seasickness had won. With his special knack of seeing opportunity in every adventure, it is reported that an agency of the U.S. government was able to put the wooden-hulled boat to good use.

Robertson returned to Chillicothe, where he founded Telesis as an invention-on-demand laboratory that produced as many as 50 unique products per year. Early patents involved data entry terminals and electrostatic length measurement devices. Some of his more fun projects included controlling electrostatic discharge from hovering helicopters and electronic tuners for steel guitars. Eventually Telesis found its niche focusing on product marking and traceability.

In 1993 Robertson sold Telesis and, along with 13 employees who loved custom design, founded InfoSight. Robertson pioneered innovative applications of lasers and ceramics, that together with unique capabilities in custom automation have made InfoSight known around the world as the people who "barcode difficult stuff."

In 2018 Robertson achieved his dream of leaving a legacy for the employees of Infosight by completing the transition to being 100 percent employee owned.

Ceramics provider purchases L&L floor-standing box furnace

L&L Special Furnace Co., Inc. shipped a floor-standing, high-temperature silicon carbide furnace to a leading worldwide supplier of high-temperature piezo ceramics used in the military, aerospace, and medical fields.

The L&L model GLF836 has an effective work zone of 18" wide by 18" high by 36" deep. The furnace has a double pivot horizontal door. It is used for processing glass products to 2,500°F / 1,371°C. This process causes lead to outgas from the process. The furnace interior is constructed from high-alumina refractory with less silica than normal linings, which helps delay the corrosive reaction between the silica present in the refractory and the lead outgassing at elevated temperatures. There is also a removable layer of recrystallized alumina fiber board in the hot zone. This sacrificial high-alumina board can be removed and easily replaced, which helps maintain the furnace chamber integrity.

The furnace is powered by high-density, silicon-carbide elements located above and below the furnace hearth. It is controlled by a SOLO single-set point control with over-temperature protection. A tap transformer is included with multiple taps to adjust the primary element voltage as needed as the heating elements change in resistance. An SCR power control with soft start regulates the output voltage to the elements.

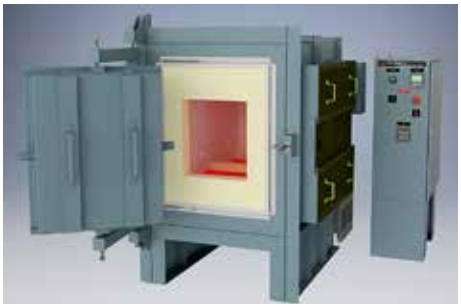

Rendering of Model GLF836 high temperature box furnace. (Courtesy: L&L Special Furnace Co.)

The model GLF836 features a free-standing NEMA12 control panel with fused disconnect, and Type R thermocouple for instrumentation. The furnace is also constructed to NFPA86 guidelines for safety.

Options include a variety of control and recorder configurations. A three-day, comprehensive startup service can be included with each system within the continental U.S. and Canada. International startup and training service is available by factory quote.

MORE INFO www.llfurnace.com

Ipsen USA appoints CSO to accelerate aftermarket growth

Ipsen has hired John Dykstra as chief service officer, an executive-level addition to the furnace manufacturer's U.S. leadership team.

Dykstra comes to Ipsen from Key Technologies, where he served as director, Service Operations Americas & Asia Pacific. Prior, he worked for Kohler Power Systems and Oshkosh Defense, where he held positions of increasing responsibility leading aftermarket teams.

In this newly created role, Dykstra is responsible for the growth of all North American Ipsen customer service business, which includes engineered retrofits, spare parts, and technical service. Dykstra's professional background and track record of accelerating organic revenue growth while also increasing customer satisfaction make

him an ideal fit for the role.

"I'm looking forward to working closely with John on enhancing Ipsen's technical service offerings for customers. By providing both world-class equipment and critical aftermarket support, our customers can expect to outperform and outlast their competition," said Patrick McKenna, Ipsen USA president & CEO.

John Dykstra

Dykstra earned a Bachelor of Arts degree from the University of Wisconsin Green Bay in organizational communication, a Master of Science in organizational leadership & quality from Marian University, and a Master of Business Administration from St. Norbert College. He also served for eight years in the U.S. Army.

MORE INFO www.ipsenusa.com

Growing HeatTek acquires two additional facilities

HeatTek, manufacturer of ovens, furnaces, and washers has purchased an additional facility in Ixonia, Wisconsin. This new building will serve primarily as a distribution center for the rapidly growing company's components and spare parts inventory.

This expansion is on the heels of another plant acquisition in the nearby city of West Allis, which was finalized earlier this year. The West Allis plant has three bays that provide more than 150,000 square feet of manufacturing space, a combined 400-ton crane capacity, and a specialty stainless steel bay.

"Many of our customers serve critical industries and are seeing historically high demand. HeatTek has committed to support them," said Jason Plowman, president of HeatTek. "Because of our equipment's large size, floor space is an important asset, so investing in new facilities is essential."

HeatTek's original location will remain home to its headquarters offices, R&D lab, and more than 70,000 square feet of manufacturing space. Plowman said, "The recent expansion has tripled our capacity and optimized our manufacturing process so we can support these crucial industries."

MORE INFO www.heattek.com

Gasbarre commissions mesh belt annealing line

Gasbarre Thermal Processing Systems announced the commissioning of a 24-inch wide, three zone mesh belt annealing furnace to a Midwest manufacturer of brass components. The brass annealing furnace is designed with a maximum operating

temperature of 1,650°F with a capacity of 800 lbs/hr, and uses a blend of nitrogen and hydrogen atmospheres. The system incorporates an Allen-Bradley PLC and HMI with automated atmosphere and water temperature control and datalogging. The integrated dewpoint meter ensures precise process control for consistent and reliable part quality. Gasbarre was selected as the equipment manufacturer based on their expertise in material processing and responsiveness to service the end user. The new furnace purchase was justified based on improved energy efficiency, reduced atmosphere consumption, and superior part quality against an older, existing furnace.

With locations in Livonia, Michigan; Cranston, Rhode Island; and St. Marys, Pennsylvania; Gasbarre Thermal Processing Systems has been designing, manufacturing, and servicing a full line of industrial thermal processing equipment for nearly 50 years. Gasbarre's equipment is designed for the client's process by experienced engineers and metallurgists.

MORE INFO www.gasbarre.com

Elvial S.A. purchases a second furnace from Nitrex

Elvial S.A., one of the largest aluminum extrusion companies in Greece, has purchased a second NX-815 E furnace from Nitrex Metal to meet the needs created by its plant.

"This additional NX-815 E furnace, which was installed and began production in July 2021, will help increase the production of building materials by the company," said Marcin Stoklosa, project manager at Nitrex. "The first furnace has been operational since 2016."

An Elvial representative cited good equipment, technology, and service to explain why Elvial chose to do business with Nitrex once again, said Stoklosa.

The NX-815 E is a retort furnace used for extrusion. It operates with NX Connect software, and uses the NITREG®-C (nitrocarburizing) and NITREG® (gas nitriding) technologies for dies extrusion. The machine is equipped with air conditioning, an INS series exhaust gas neutralizer, and racking of 750 kg made from Inconel 600. The order also included a lifting device. All processes for this furnace are compliant to AMS 2759/10.

Elvial S.A. is one of the largest aluminum extrusion companies in Greece. It produces integrated aluminum systems for both architectural and industrial use in a fully vertically integrated production line housed in a new state-of-the-art plant in Kilkis, Northern Greece. Elvial S.A.'s aluminum systems are certified from renowned international institutes, as well as acknowledged Greek certification bodies.

MORE INFO www.nitrex.com
www.elvial.gr

IFHTSE
INTERNATIONAL FEDERATION OF HEAT TREATMENT AND SURFACE ENGINEERING

Deadline approaching for ECHT2022 conference abstract submissions

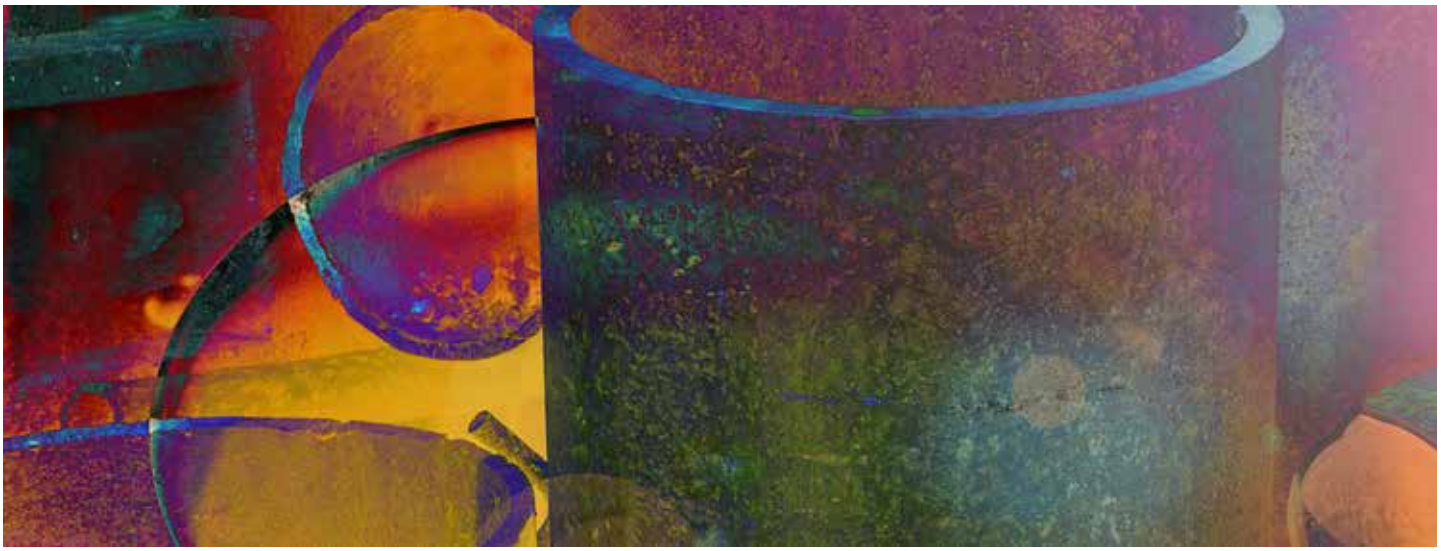

The special emphasis of ECHT2022 will be on Heat Treatment in Steel Processing.

Abstract submission deadline is January 31, 2022, for the 27th IFHTSE Congress in Salzburg, Austria, September 5-8, 2022, at the Wyndham Grand Salzburg Conference Center. Please submit your abstracts (300-400 words) via the conference website at www.ifhtse-echt2022.org.

The special emphasis of ECHT2022 will be on Heat Treatment in Steel Processing. Topics include furnace design, thermomechanical treatments, quenching technology, additive manufacturing, and coating technologies.

FORMER IFHTSE PRESIDENT PETER MAYR DIES

Former IFHTSE president, IFHTSE fellow, and director of member institute IWT, Prof. Dr.-Ing. habil. Peter Mayr, unexpectedly passed away at 83 on October 20, 2021.

With a degree in physics from Stuttgart, Germany, he conducted research in the field of the fatigue behavior of metallic materials during and after his Ph.D. in Karlsruhe, Germany.

In 1981, he became director of the then "Institut für Härterei-Technik" in Bremen as successor to Prof. Otto Schaaber, one of the "Founding Fathers" of IFHTSE. In his 20-year tenure, Mayr laid the foundations for today's Leibniz-IWT by expanding the scope of the institute, renamed "Institut für Werkstofftechnik IWT" (Institute for Materials Technology). He established the independent departments "Manufacturing Technologies" and "Process Engineering." In 2000, the collaborative research center "Distortion Engineering" was initiated. This research center had its focus on understanding the interdependence of all factors for dimensional stability of heat-treated components along the entire process chain. Long before any eventual distortion upon heat treatment, the part acquires a "distortion potential" during the prior processing steps — a term specifically created in this context. The success of this research earned him the IFHTSE Fellowship in 2007 "In recognition of a wide range of research and development contributions to many aspects of heat treatment, most notably in the study of distortion." The ample results of this research center were presented and discussed in the conference series "IDE (International Distortion Engineering)," which was merged in 2015 with IFHTSE's series "QCD (Quenching and Control of Distortion)" to form "QDE," held in Berlin, Germany, and Kyoto, Japan). From the beginning, Mayr was also editor-in-chief of HTM, the leading German-language heat-treating technical and scientific journal.

Peter Mayr

While he took more functions in a considerable number of organizations of collaborative research, Mayr became a personal hub of

cooperation, communication, and contacts in the research landscape, taking leadership positions in many other technical organizations. He was appointed to the German Science Council in 1997 by the president of the Federal Republic of Germany. This commitment was not limited by the national borders, as proven by his service as IFHTSE president from 1996 to1997.

He had an affable and approachable personality with a sense of humor. He was always full of ideas and projects. His extensive expertise and great experience ensured his advice was always helpful.

We shall always hold his memory in honor.

HISTORICAL IFHTSE CONFERENCE PROCEEDINGS

IFHTSE has a 50-year history in organizing international events across the globe. Unfortunately, the past congresses were not archived electronically due to unavailable technology at that time. IFHTSE is endeavoring to capture those older papers by scanning the conference proceedings and placing them on our website for posterity. At the present time, there are approximately 27 programs and proceedings available at www.ifhtse.org.

MEMBER SPOTLIGHT

IFHTSE is a federation of organizations not individuals. There are three groups of members: scientific or technical societies and associations, universities and registered research institutes, and companies.

In this segment, we will highlight our members. This month we highlight the Chinese Heat Treatment Association. The current president is Li Xinya of the Machinery Research Institute, Ltd. The Chinese Heat Treatment Association was founded in 1986. It is a non-profit industrial organization composed of companies (and related production), research institutes, and organizations in the heat-treatment industry throughout China. CHTA, with its thousands of members, is active in heat treatment and surface engineering. They produce a series of practical heat-treatment courses often led by international experts in the field.

The scope of the Chinese Heat Treatment Association is to promote reasonable policies from the government for the entire heat-treatment industry. This is further expanded by organizing experts to draft, revise, and review industry standards and regulations. CHTA is actively involved with disseminating information to its member companies and members on new technologies, processes, and equipment. For more information, go to www.chta.org.cn.

IFHTSE 2022 EVENTS

APRIL 25–27, 2022
12th Tooling Conference & Exhibition (Tooling 2022)
Örebro, Sweden | www.tooling2022.org

JUNE 19–23, 2022
6th International Conference on Steels in Cars and Trucks
Salzburg, Austria | www.sct-2020.com

SEPTEMBER 5–8, 2022
27th IFHTSE Congress / European Conference on Heat Treatment
Salzburg, Austria | www.ifhtseecht2022.org

APRIL 21–24, 2023
5th International Conference on Heat Treatment and Surface Engineering of Tools and Dies
Liangzhu Dream Town, Hangzhou, China

MAY 2023
European Conference on Heat Treatment
Italy

NOVEMBER 13-16, 2023
28th IFHTSE Congress
Yokohama, Japan

For details on IFHTSE events, go to www.ifhtse.org/events

IFHTSE LEADERSHIP

EXECUTIVE COMMITTEE

Eva Troell | President
RISE IVF Research Institutes of Sweden | Sweden

Dr. Scott MacKenzie | Past President
Houghton International Inc. | USA

Prof. Masahiro Okumiya | Vice President
Toyota Technological Institute | Japan

Dr. Stefan Hock | Secretary General
IFHTSE Italy

Dr. Imre Felde | Treasurer
Óbuda University | Hungary

OTHER MEMBERS

Prof. Rafael Colas | Universidad Autónoma de Nueva Leon | Mexico
Dr. Patrick Jacquot | Bodycote Belgium, France, Italy | France
Prof. Massimo Pellizzari | University of Trento | Italy
Prof. Larisa Petrova | MADI University | Russia
Prof. Reinhold Schneider | Univ. of Appl. Sciences Upper Austria | Austria
Prof. Marcel Somers | Technical University of Denmark | Denmark
Prof. Kewei Xu | Xi'an University | China

ONLINE www.ifhtse.org | **EMAIL** info@ifhtse.org

Cruise into 2022: IHEA's annual meeting sets sail in March

IHEA's four-day Annual Meeting event will feature two sea days aboard Royal Caribbean's Brilliance of the Seas and a day in Costa Maya.

IHEA is in full preparation mode for the 2022 Annual Meeting aboard Royal Caribbean's *Brilliance of the Seas*. This will be the third time IHEA will hold an Annual Meeting on a cruise ship.

"We are very excited to finally be able to meet once again onboard a ship," said IHEA's Executive Vice President Anne Goyer. "I've been able to personally sail recently, and I believe this is the safest place to hold our next annual meeting. The ship is cleaned constantly, and their health and safety protocols are strictly adhered to. We look forward to welcoming everyone to IHEA's 92nd Annual Meeting in March."

This four-day event will feature two sea days and a day in Costa Maya. This budget-friendly meeting allows both the members and the association to reduce expenses over a land-based resort as the cruise lines include meeting items that land-based hotels charge for. Registration fees for this meeting are greatly reduced. Depending on the cabin type you choose, members can save between 20 and 30 percent over traditional annual meeting costs.

IHEA has an outstanding program planned with timely and important presentations as well as plenty of time for social interaction during receptions, meal functions, and, of course, a cruise ship mini-golf tournament.

CYBERSECURITY FOR THE INDUSTRIAL HEATING INDUSTRY

Jason Floyd, Ascent Solutions

As automation continues its manufacturing growth along with the ability to control our processes from just about anywhere in the world, cybersecurity becomes more important each and every day. Companies cannot afford to have their manufacturing lines disrupted by cybersecurity attacks. In this presentation, Jason Floyd will review the importance of having the proper cybersecurity plans in place for manufacturing and the industry along with

IHEA 2022 ANNUAL MEETING TOPICS

CYBERSECURITY FOR HEAT TREATERS

2022 ECONOMIC FORECAST

HYDROGEN COMBUSTION

what you can do if a cybersecurity attack happens.

ECONOMIC UPDATE: WHERE ARE WE HEADED IN 2022 AND BEYOND?

Chris Kuehl, Armada Corporate Intelligence

An annual favorite, IHEA's economist Chris Kuehl will join us to give an economic update with his take on what lies ahead in 2022. As our economic uncertainties continue, Kuehl will join us to review the latest economic data and influencers in his popular, informative, and entertaining manner. He will break down where the economy stands in early 2022 while forecasting where he believes we are going throughout the rest of the year and beyond.

Jason Floyd

Chris Kuehl

THE GREAT DEBATE: HYDROGEN COMBUSTION

Tim Lee, Honeywell Thermal Solutions
Joe Wünning, WS Thermal Process Technology Inc.
Dave Schalles, Bloom Engineering

The hottest topic (no pun intended) right now is hydrogen combustion and how the industrial heating equipment industry is preparing for the future as it relates to these technologies. How will your company prepare? What long-term impact will this have on IHEA members and our industry? To help members better understand where things are headed, we've assembled a panel of experts to host an interactive session on this important issue for all IHEA members.

The programming content combined with the social activities will deliver an outstanding 92nd Annual Meeting. Register at www.ihea.org/event/AM22.

IHEA 2022 CALENDAR OF EVENTS

JANUARY 17–FEBRUARY 27

Fundamentals of Industrial Process Heating online course

This course is designed to give the student a fundamental understanding of the mechanisms of heat transfer within an industrial furnace and the associated losses and the operation of a heating source either as fuel combustion or electricity. All concepts are derived mathematically with limited use of "rules of thumb."

Online registration is available until January 13

FEBRUARY 15–16

Powder Coating & Curing Processes Seminar

The day and a half Introduction to Powder Coating & Curing Processes Seminar will include classroom instruction and hands-on lab demonstrations.

Alabama Power Technology Applications Center I Calera, Alabama
Registration Fee: IHEA members: $325 / Non-members: $425

MARCH 14–17

Electrification 2022 International Conference & Exposition

This event will share what's new in the electrification of buildings, vehicles and industry. Spend time with your colleagues and explore efficient, equitable solutions for a net-zero economy.

Charlotte Convention Center I Charlotte, North Carolina

For details on IHEA events, go to www.ihea.org/events

INDUSTRIAL HEATING EQUIPMENT ASSOCIATION

P.O. Box 679 I Independence, KY 41051
859-356-1575 I www.ihea.org

D. SCOTT MACKENZIE, PH.D., FASM
SENIOR RESEARCH SCIENTIST–METALLURGY /// QUAKER HOUGHTON INC.

The compatibility of different metallic and non-metallic materials with polymer quenchants is generally good; however, specific combinations should be tested before application.

Compatibility of polymer quenchants with metals, seals

In this column, I will discuss the compatibility of polymer quenchants and materials used in the construction of quench tanks, heat exchangers, and pump seals.

Polymer quenchant products are concentrated, oil-free quenchant bases. They dissolve easily in water and are used in concentrations from two percent to 40 percent depending upon the quenching speed desired. The products are primarily used for quenching steel, aluminum, and titanium alloys. As systems in use will consist of 60 percent to 98 percent water with a few exceptions, materials used must be compatible with water.

Polymers will be mixtures of water and polyalkylene glycol (PAG), water and polyvinyl pyrrolidone (PVP), water and sodium polyacrylate (ACR), or water and poly(2-ethyl-2-oxazoline) (PEOX). There are other quenchants that are mixtures of these polymers in various amounts. In addition to the primary polymer, there are other additives, such as pH booster, corrosion inhibitors (steel and yellow metal), and other packages that provide specific capabilities, such as biostability. Each of these polymers and additive packages has specific compatibility to metallic and non-metallic materials.

METALLIC COMPATIBILITY

Most quenching systems are manufactured of low carbon steel such as boiler plate with similar or other metals used in the piping, cooling, and agitation systems.

›› **Steel:** Generally, all polymer quenchants have ferrous corrosion inhibitors present to make the products compatible with steel.

›› **Aluminum:** Unanodized aluminum is not considered compatible as it will corrode during long-term immersion. Anodized aluminum is compatible to a certain extent. It is like results obtained with plain water. Aluminum pump accessories are not compatible, as erosion occurs due to wear actions. Due to high pH, staining of aluminum may occur during prolonged exposure. Therefore, it is always recommended to rinse off excess polymer with water after quenching aluminum.

›› **Copper:** Is compatible with polymer quenchant systems with a few exceptions. Ammonia-containing atmospheres have the ammonia dissolved into the water. This ammonia water solution corrodes copper vigorously. In such circumstances, replace copper-type cooling coils and accessories with steel. Brass is compatible but leaded brass should be avoided. Yellow metal corrosion inhibitors are often added to polymer quenchants to minimize corrosion. A solution that turns blue after time could be indicative of inadequate yellow metal corrosion inhibitors present in the quenchant, and may need a corrosion inhibitor boost.

›› **Cadmium, lead, magnesium and zinc:** Are not compatible with polymer quenchant solutions.

›› **Cast iron and ductile irons:** Rust more easily than steel. They should be coated with a compatible inhibitor prior to use. Additional corrosion inhibitors may need to be added to the solution to boost pH and minimize corrosion.

NON-METALLIC COMPATIBILITY

Rubber and seal materials can react differently to different liquids.

In the case of specific or uncovered product compatibility, the polymer quenchant supplier should be contacted. Compatibility tests can usually be conducted by the polymer producer, or they have already performed the necessary compatibility tests.

Different temperatures and exposure times can produce acceptable results under one set of conditions but result in failure under different conditions. Typically, these seal materials change volume by swelling. This can affect the performance of the product. Other non-metallic materials may degrade by exposure to the polymer quenchant.

Compatibility is usually measured by swell testing, by such test methods as "ASTM D471—Standard Test Method for Rubber Property—Effect of Liquids," or "ISO 1817—Rubber, vulcanized or thermoplastic — Determination of the effect of liquids." These test methods measure the degradation or swelling of the liquid/rubber (or polymer) pair.

Cork and leather are not compatible with polymer quenchant solutions. Swelling will most likely occur.

» **Rubber:** Buna N, Neoprene, Butyl, E.P.R., Fluorosilicone, Teflon, Viton, and Corfam are compatible within the temperature limitations listed by their manufacturer. Polyurethane rubber is not compatible with most polymer quenchants.

» **Plastics:** Acrylic, epoxy, Lucite, nylon, phenolic, polyethylene, PVC, silicone, and styrene are compatible within the temperature limitations given by the plastic supplier.

» **Screen material:** Cloth, cotton, and nylon are compatible. Review specific metal for metallic screen compatibility.

» **Filter media:** Diatomaceous or Fuller's earth type, absorbent media is not compatible, nor are untreated cellulose media. Phenolic-treated cellulose is compatible, along with various plastic media. Sand filters are usually recommended for polymer quenchants because of the effectiveness and low cost of filter media.

» **Paint:** Epoxy and phenolic paints are compatible within temperature limitations listed by paint suppliers. Alkyd, polyurethane, and other industrial paints are not compatible. Lifting of paint often occurs. Sprayed-on truck bed liner materials have been used successfully by some users. It is good to test compatibility prior to extensive use.

In the case of specific or uncovered product compatibility, the polymer quenchant supplier should be contacted. There are many other different types of materials not covered here. Compatibility tests can usually be conducted by the polymer producer, or they have already performed the necessary compatibility tests. After exposing the seal material to the liquid, the properties of the seal material are measured. Often this includes the volume change, tensile properties (ultimate strength and elongation), and the hardness of the exposed material, as measured by a durometer.

CONCLUSION

The compatibility of different metallic and non-metallic materials with polymer quenchants is generally quite good. However, specific combinations of materials should be tested prior to application, or the manufacturer of the quenchant or material can be asked to perform swell testing of the specific product couple.

As always, should you have comments on this column, or suggestions for any other columns, please contact the writer or editor.

ABOUT THE AUTHOR

D. Scott MacKenzie, Ph.D., FASM, is senior research scientist-metallurgy at Quaker Houghton. He is the past president of IFHTSE, and a member of the executive council of IFHTSE. For more information, go to www.houghtonintl.com.

TONY TENAGLIER
HEAT TREAT PROCESS ENGINEER ///
HITCHINER MANUFACTURING

Motivation comes from several directions, and transforming work into mini challenges presents workers a chance to use their skills to achieve success and feel invested.

Set company goals that engage employees daily

It's a new year. A chance to start fresh. A chance to set the entire year's goals for yourself, the department you work for, and the company. However, there are other goals aside from the standard KPIs (key process indicators) that are often overlooked or not even considered.

As a soccer player knows, the goal each season is to win as many games as possible. During each game, both teams try to score as many points as possible and they have a set amount of time to do it. Equally, an employee understands lowering scrap defects and improving on delivery to customers each quarter, and over the course of the year that gets them to a winning season. But what about the weekly goals? The daily goals? The goals each hour and minute of each day? Aside from the reports needed to generate for scrap or showing up to work on time each day, what other goals should employees be setting?

Motivation comes from three different things that drive someone to do what they do. In no order, the first is biological drive — for example, needing food. The second is extrinsic reward, based upon rewards and punishments. The third is intrinsic reward. Motivation is what moves a person toward a goal. A runner is motivated to cross the finish line, maybe in the fastest amount of time. Maybe it is to beat all the other runners that day. Maybe it's just to finish the race to simply prove they could do it. Maybe it was to earn a medal for completion.

A company sets up the extrinsic rewards with a paycheck based upon KPIs being met, knowing this is often a good motivation technique. The potential medal earned at a company and this structure is a metric for a company to grow. These extrinsic rewards help "finance" biological motivations for an individual. However, more qualitative measures of intrinsic motivations are not always made clear or are overlooked at a company and those also are a factor in employee success. The Sawyer Effect, based upon Mark Twain's novel of young Tom Sawyer, is an example where intrinsic motivation can be found even in places where we might not expect it.

As the story goes, Tom has been punished and is required to paint a lengthy fence. He doesn't want to do it but knows that he must. As his friends walk by, he is embarrassed at first by what they might think. But then he turns it into a game, trying to convince them to want to paint the fence for him. Tom is able to get his friends to not only paint the fence, but also give him gifts for doing it!

Work has been transformed into play. A seemingly routine (and arduous) task becomes something his friends now actually want to participate in. This is the goal for employees who want to excel, cultivating this intrinsic motivation. Employees know they must work to earn a paycheck — part of the overall motivation for an employee. Employees also know that this hard work pays off to provide for a family, afford food and shelter (and a car, bills, CD rewinder, beach sombrero, etc.). What everyone doesn't realize is that work doesn't always have to be viewed as a big drag.

Tom's strategy was simple. He created a mini game in the overall game he was playing — needing to get the fence painted. He made it seem like his friends were missing out on something. Whether it be the implication that only exclusive kids got to paint the fence, or the potential of them missing out on the experience of such a rare task, the overall feeling (whether it be jealousy, curiosity, or a chance to prove one's own worth) created a challenge. People like challenges, as sometimes the goal can be made clearer.

Painting a fence is pretty easy. With proper technique of the paint brush and a full can of paint, it can be done. It can be scheduled into a preventive maintenance program for a consistent frequency for the next year or two. However, the way it is being done can affect the overall quality of how it gets done. Regardless of dictating tight requirements such as measurement of each paintbrush stroke's distance from the next, even such rigorous tolerances on a task don't put in place what is needed for an employee to perform the job successfully. Tight measures are a way to track quality, but sometimes are more valued than the way the work is presented, which should be a goal as well. Instead of simply assigning tasks for employees to work, a better strategy for more engagement and more productivity might be found in creating an environment where employees can use their skills to overcome a challenge. Instead of being assigned a task, it's seen more as an opportunity. But how can you convince an employee to do that? If you evoke a challenge, some employees might even get upset.

Therefore, it is important to cultivate mini games throughout the day, because the tasks sometimes become unclear. On the surface, a seemingly arbitrary task has no value in an employee's life other than earning a paycheck. Acting like an employee zombie does earn a paycheck but doesn't improve the employee's overall happiness. This dissatisfaction can reach a threshold that could result in an employee not being engaged and possibly quitting.

In psychology, there is a term that refers to a specific personality type for those who view a challenge as either a potential success or potential failure: an autotelic personality. Couple this personality type of viewing challenges every day with a mindset that converts work to play, and you have a more effective employee who can better understand and navigate their day. They will not only see challenges as potential outcomes for success but manage to turn the task into a "game." The company loves to win at the game and employees will feel more successful when they win more each day.

ABOUT THE AUTHOR

Tony Tenaglier is the heat treat process engineer at Hitchiner Manufacturing. He earned both a B.S. in material science engineering and an M.A. in psychology. You can contact Tenaglier at tony_tenaglier@hitchiner.com.

THERMAL PROCESSING MEDIA PORTAL

Thermal Processing's online portal is your gateway to social media news and information resources from manufacturers and service providers in the heat-treating industry. You'll find links to social media as well as webinars, blogs and videos.

This quick-and-easy resource is just a click away at thermalprocessing.com.

Thermal processing

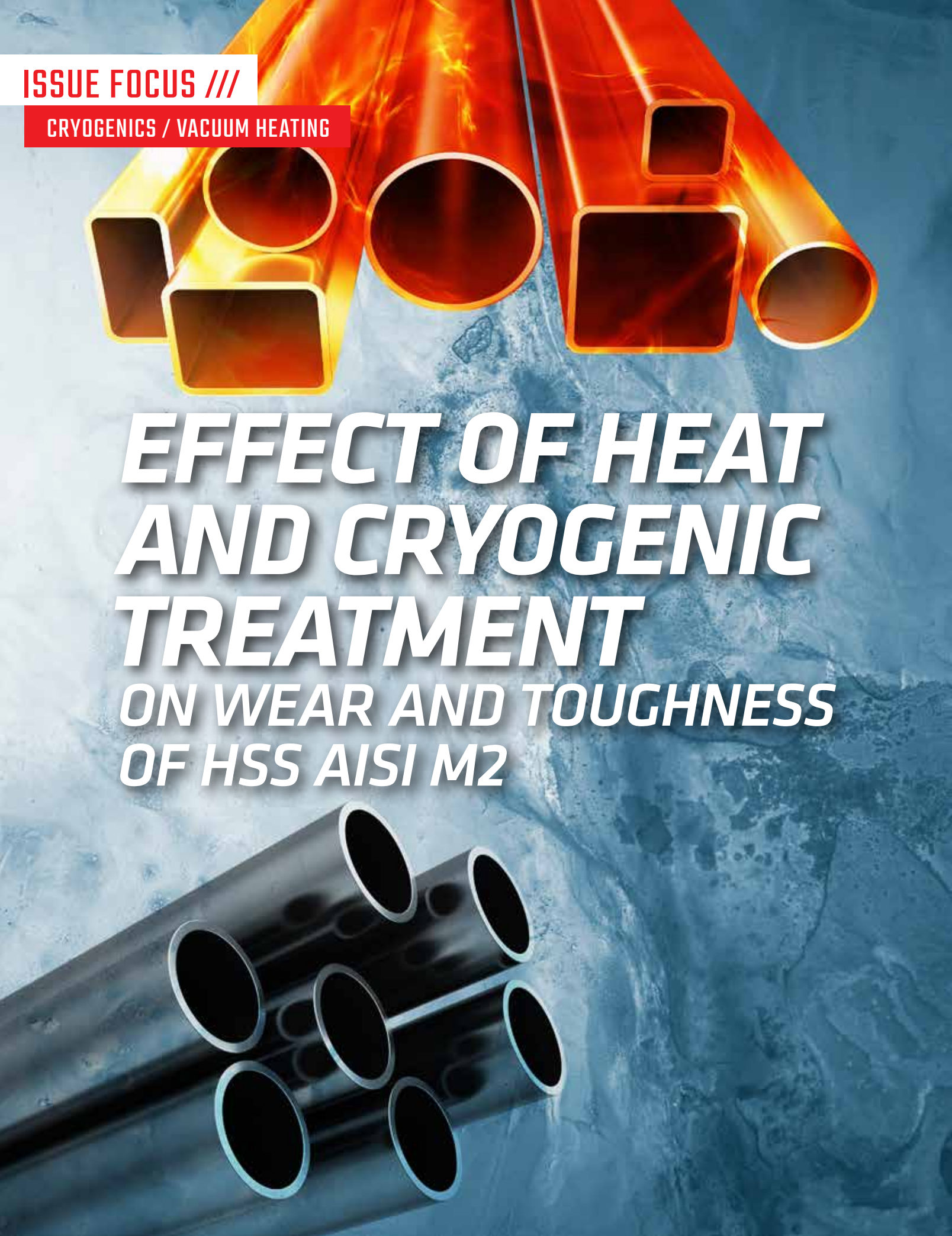

EFFECT OF HEAT AND CRYOGENIC TREATMENT ON WEAR AND TOUGHNESS OF HSS AISI M2

Cryogenic treatment should not be considered only as an add-on process to quenching and tempering but rather should be designed simultaneously.

By DIEISON G.FANTINELI, CLEBER T.PARCIANELLO, TONILSON S.ROSENDO, AFONSO REGULY, and MARCO D.TIER

Despite the promising results obtained with cryogenic treatment of tool steels, there are still contradictions regarding its benefits, and there is no consensus regarding its mechanisms in the steel microstructure. The goal of this work is to investigate the optimum heat treatment process parameters together with the cryogenic treatment. Samples of AISI M2 steel were austenitized at 1,170, 1,200 or 1,230°C and quenched in salt bath. The cryogenic treatment was performed through nitrogen nebulization with a cooling/heating rate of 0.3°C/min, 24-hour holding time at minus-190°C, before, after or between the double tempering. The influence of cryogenic treatment in AISI M2 steel was dependent on the previous austenitization temperature. No significant reduction in retained austenite was observed by deep cryogenic treatment. The benefits achieved in the resistance to abrasive wear and toughness are associated with a lower amount of carbon in the martensite, together with finer and more homogeneous carbide precipitation.

1 INTRODUCTION

High speed steels (HSS) comprise an important group of materials for tool manufacturing. Among these materials, AISI M2 steel stands out due to its high hardenability, high wear resistance, and good toughness. These properties are associated with a martensitic structure of high thermal stability reinforced with carbides of chromium, molybdenum, tungsten, and vanadium [1].

To obtain an extended tool life, the choice of steel type alone is not sufficient. Additionally, the selection of suitable parameters for the heat treatments is of major importance. Research conducted in the last three decades indicates the abrasive wear resistance of metal alloys may increase substantially with the application of cryogenic treatments [2].

Cryogenic treatment (CT) is performed by controlled cooling of the material at temperatures ranging from minus-80 to minus-196°C followed by holding at the cryogenic temperature for a period of time. It is classified as shallow cryogenic treatment (SCT) when temperatures up to minus-80°C are applied (dry ice temperature) and deep cryogenic treatment (DCT) when temperatures close to liquid nitrogen are reached (minus-196°C) [3]. CT does not replace quenching, tempering, or any other conventional heat treatment but is a complement to other process procedures.

Two metallurgical phenomena are reported as major reasons for the benefits associated with DCT. First, the elimination of the retained austenite; and second, the precipitation of a large amount of extremely fine carbides [4]. For temperatures close to minus-80°C, there is a transformation of a significant portion of retained austenite to martensite [5], and for temperatures close to minus-196°C, the treatment causes the formation of fine carbides, considered the main factor responsible for the increase in wear resistance [6]. Amini et al. [7] report DCT promotes an increase in the carbide percentage and precipitation of more homogeneous nano carbides.

A matter that needs to be clarified is how this precipitation occurs during DCT because the diffusion of the carbon atoms decreases exponentially with the decrease in temperature. Akhbarizadeh and Javadpour [8] concluded the as-quenched vacancies play an important role in the carbide formation during DCT by providing appropriate sites for the carbon atoms jumping.

After the study of influence of process parameters, Darwin et al. [9] report the main influencing DCT are soaking temperature,

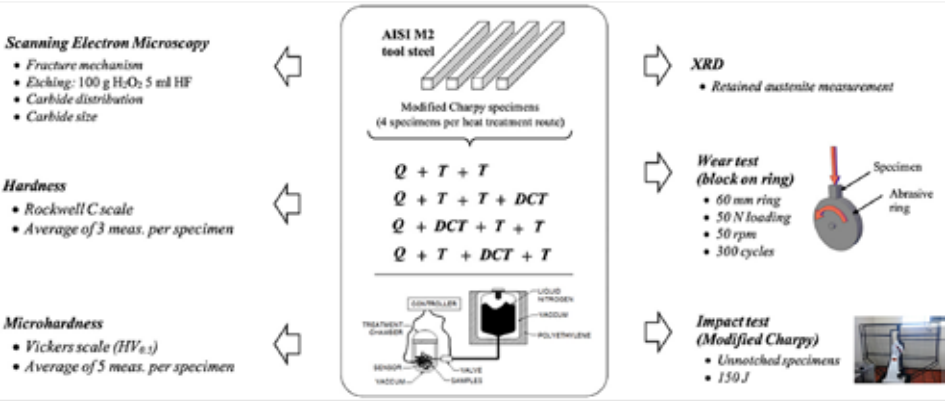

Figure 1: The main stages of the experimental procedure.

Element	C	Cr	V	W	Mo
% WT	0.87	3.75	2.05	7.65	4.71

Table 1: Chemical composition of the AISI M2 assessed by optical emission spectroscopy.

soaking period, and cooling rate. Furthermore, Baldissera and Delprete [3] report that holding periods above 36 hours do not result in benefits, and that, in most cases, 24 hours are sufficient to reach optimal results. Direct immersion in liquid nitrogen has already been widely used. The main advantage is the simplicity of the equipment. In addition, the temperature of minus-196°C is actually achieved because the material makes direct contact with the liquid nitrogen. However, the cooling rate is very high, resulting in embrittlement of the material. Therefore, Molinari et al. [10] report one of the most critical parameters is the cooling rate, which should not exceed 0.5°C/min.

Senthilkumar and Rajendran [11] performed a review and reported DCT can improve the wear behavior, toughness, corrosion resistance, tensile and fatigue properties of steels. However, some

researchers are skeptical about DCT because of the lack of visualization of the microstructural changes as discussed by Mohan Lal et al. [12]. Differences in the results from different studies can be explained first by differences in the process. For instance, some studies such as Podgornik et al. [13] performed the cooling down to cryogenic temperature by direct immersion in liquid nitrogen at a cooling rate of 300°C/min. Furthermore, Das et al. [14] showed the effect of DCT is dependent on the mode and mechanisms of wear. Therefore, the differences in the type and parameters of the wear test may also explain the differences in the wear performance.

In this context, the main objective of this research is to investigate the influence of the austenitization temperature and the annealing cycles on the effect of DCT in relation to the mechanical and tribological properties of an AISI M2 steel. The cryogenic and heat-treatment parameters were correlated to each other.

2 MATERIALS AND METHODS

Figure 1 illustrates the main stages of the experimental procedure.

Table 1 presents the chemical composition of the HSS AISI M2 investigated in this work and supplied by Favorit Steels (Cachoeirinha, RS – Brazil). The samples were machined to the dimensions of the Charpy specimen (10 × 10 × 55 mm) without notch in quadruplicate. The following parameters were used for the heat treatments: austenitizing temperature, 1,170, 1,200 or 1,230°C; quenching in a salt bath at a temperature of 500°C; double tempering at 550°C for 120 minutes each. DCT was performed at minus-190°C for 24 hours with nitrogen nebulization and a 0.3°C/min cooling/heating rate. Figure 2 illustrates the cryogenic system.

Table 2 presents the sample identification and its heat-treatment parameters. The first four digits indicate the austenitization temperature. "DCT" indicates the presence of the deep cryogenic treatment, and "R" or "2R" indicate simple or double tempering. The identification sequence permits the determination of whether DCT was performed before, after, or between the tempering processes.]

The analysis of the distribution and size of carbides was performed by scanning electron microscopy (SEM) after the sample etching by hydrofluoric acid solution (100 g H2O2 5 ml HF) for 40 seconds.

An X-ray diffraction (XRD) technique was used to retained austenite measurements in a GE — Seifert Charon XRD M — Research Edition equipment and Rayflex Analyze 2.503, module austenite/nitrate software. The measurements were performed with Cr k-alpha radiation (2.2897 Å), 30 kV–50 mA, vanadium k-beta filter, meteor 1D detector, 0.02°step/500 second time, 55-166°, 2 mm collimator.

The evaluation method is based on the calculation of the integral intensities of measured peaks and are finally put in proportion via special intensity factors according to Equation 1. The peaks used for calculations was A110, A200, A211 for ferrite, and G111, G200, G220 for austenite:

$$Q = \frac{100\%}{\frac{J_a}{J_g} * \frac{R_g}{R_a} + 1}$$

For the assessment of the mechanical properties, the Rockwell C (HRC) hardness, Vickers microhardness ($HV_{0,5}$) and Charpy impact tests with a 150 J hammer were performed. The fracture mechanisms of the impact tested samples were assessed by SEM.

The abrasive wear test was performed in the block-on-ring configuration, schematically shown in Figure 3 using the following parameters: 60 mm diameter disc with contact face covered with 120 grit sandpaper (replaced after each test), 50 N load, 50 RPM speed (0.15 m/s) and 300 revolution cycles.

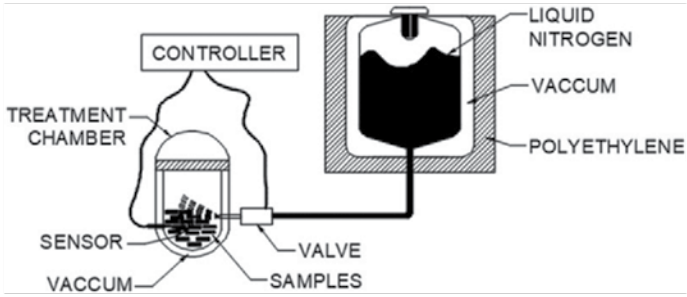

Figure 2: Cryogenic system used in this work.

Sample identification	Austenitizing temperature	(DCT)	DT[a] after quenching	DT[a] after DCT	Tempering before and after DCT
1170/2R	1170°C	NO	YES	NO	NO
1170/2R/DCT	1170°C	YES	YES	NO	NO
1170/1R/DCT/1R	1170°C	YES	NO	NO	YES
1170/DCT/2R	1170°C	YES	NO	YES	NO
1200/2R	1200°C	NO	YES	NO	NO
1200/2R/DCT	1200°C	YES	YES	NO	NO
1200/1R/DCT/1R	1200°C	YES	NO	NO	YES
1200/DCT/2R	1200°C	YES	NO	YES	NO
1230/2R	1230°C	NO	YES	NO	NO
1230/2R/DCT	1230°C	YES	YES	NO	NO
1230/1R/DCT/1R	1230°C	YES	NO	NO	YES
1230/DCT/2R	1230°C	YES	NO	YES	NO

[a] DT indicates double tempering

Table 2: Heat Treatment Routes.

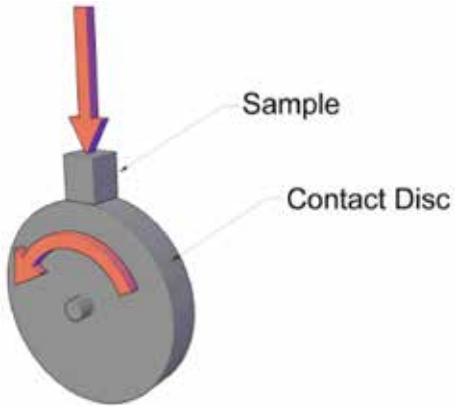

Figure 3: Wear test configuration: Block on ring.

3 RESULTS

3.1 Hardness

The HRC hardness measurements, performed after tempering, shown in Figure 4 that the heat treatment procedure was properly performed, with an average hardness above 63 HRC.

For the three austenitization temperatures analyzed, the highest values of hardness and lowest values of standard deviation were reached when DCT was applied before the tempering. The statistical analysis of the measurements shows an increase in HRC hardness

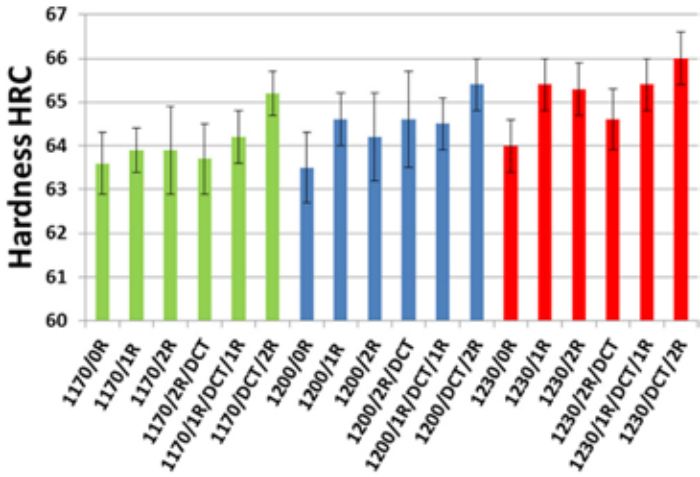

Figure 4: Hardness HRC for different heat treatments.

when DCT is applied before tempering, as the increase was greater than the coefficient of variation.

Table 3 presents the HV0.5 microhardness results. Although there are signs of microhardness increasing after DCT for the austenitized samples at 1,170 and 1,200°C, it is not possible to make such an assertion because the coefficient of variation was well above the percentage of microhardness variation. When DCT was applied before tempering, a significant reduction of the standard deviation was observed, indicating a more homogeneous microstructure.

3.2 Wear test

Table 4 and Figure 5 present the results of the wear test. The samples treated by route 1200/DCT/2R showed the lowest mass loss, with a reduction of 18% over the 1200/2R route.

For the austenitization temperature of 1,230°C, there is a tendency to reduce the wear resistance, but the variations were lower than the coefficient of variation. For the austenitized temperature at 1,170°C, the wear resistance increased when DCT was applied after double tempering (1170/2R/DCT), whereas for the austenitized samples at 1,200°C, the increase occurred when DCT was performed before double tempering. These results suggest the optimal cryogenic parameters should be defined simultaneously with the quenching and tempering parameters.

Akhbarizadeh et al. [15] associate the benefits of DCT with the transformation of the retained austenite to martensite. However, in the comparison of the wear resistance for the samples treated with shallow cryogenic treatment (SCT) and deep cryogenic treatment (DCT), both having almost the same amount of retained austenite, better performance was found for DCT [16], suggesting that other factors contribute to improving wear resistance.

Figure 6 compares the amount of austenite for samples with and without DCT. Different than expected, DCT does not result in significant reduction of retained austenite. This behavior can be explained by the several weeks of time between quenched and tempering/DCT processes. According to Morgan and Ko [17] and Mohanty [18], it is possible that the phenomenon of austenite stabilization occurred.

3.3 Carbide precipitation

Figure 7 presents the carbide precipitation for the samples austenitized at 1,170°C with and without DCT. For the sample without DCT (1170/2R) the average size of carbide precipitations is 2.18 ± 0.63 μm while for sample with DCT (1170/DCT/2R) is 1.48 ± 0.45 μm as presented in Figure 8.

3.4 Impact toughness

The results presented in Table 5 and Figure 9 demonstrate the influence of the austenitization temperature and DCT on the impact toughness of the samples.

Sample	$HV_{0.5}$	Increase[a]	SD	SD variation	Coefficient of variation
1170/2R	833.5	–	33.8	–	4.1
1170/2R/DCT	831.0	-0.3%	38.8	+14.8%	4.7
1170/1R/DCT/1R	839.6	0.7%	39.9	+18.0%	4.8
1170/DCT/2R	857.9	2.9%	30.3	-10.4%	3.5
1200/2R	859.4	–	34.6	–	4.0
1200/2R/DCT	885.3	3.0%	40.6	+17.3%	4.6
1200/1R/DCT/1R	862.6	0.4%	36.1	+4.3%	4.2
1200/DCT/2R	880.9	2.5%	29.6	-14.5%	3.4
1230/2R	899.3	–	33.1	–	3.7
1230/2R/DCT	871.9	-3.0%	17.2	-48.0%	2.0
1230/1R/DCT/1R	874.3	-2.8%	27.4	-17.2%	3.1
1230/DCT/2R	879.7	-2.2%	26.5	-19.9%	3.0

[a] Compared to sample TEMP/2R

Table 3: Microhardness HV0.5.

Sample	Weight loss %	SD	Coefficient of variation	Variation of mass loss compared with TEMP/2R
1170/2R	0.293	0.033	–	–
1170/2R/DCT	0.255	0.022	9%	-13%
1170/1R/DCT/1R	0.269	0.050	18%	-8%
1170/DCT/2R	0.281	0.038	14%	-4%
1200/2R	0.291	0.018	–	–
1200/2R/DCT	0.304	0.022	7%	+5%
1200/1R/DCT/1R	0.269	0.039	14%	-7%
1200/DCT/2R	0.237	0.030	13%	-18%
1230/2R	0.277	.041	–	–
1230/2R/DCT	0.249	0.056	22%	-10%
1230/1R/DCT/1R	0.282	0.029	10%	+2%
1230/DCT/2R	0.261	0.045	17%	-6%

Table 4: Wear test.

DCT increased the impact toughness on the austenitized routes at 1,170 or 1,200°C, especially for sample 1170/1R/DCT/1R, with a 56% increase. For better statistical analysis the results from Figure 9 were grouped by the same temperature (Figure 10a), by the presence of DCT or not (Figure 10b), and by similar treatment routes (Figure 10c).

It is possible to observe that austenitizing at lower temperature and the presence of DCT resulted in higher toughness. Furthermore, DCT positioned between both tempering resulted in the highest toughness.

Figure 11 shows the grain sizes according to austenitizing temperature. At 1,170°C, the mean diameter was 7.8 ± 0.6 μm (G = 11.1); at 1,200°C, it was 8.8 ± 0.6 μm (G = 10.8); and at 1,230°C, it was 10.2 ± 0.8 μm (G = 10.3). Therefore, grain size may explain the higher toughness observed for samples austenitizing at lower temperature as observed in Figure 10a.

All of the samples presented a transgranular fracture governed by dimples as shown in Figure 12. This is a desirable indication that none of the heat-treating routes caused embrittlement.

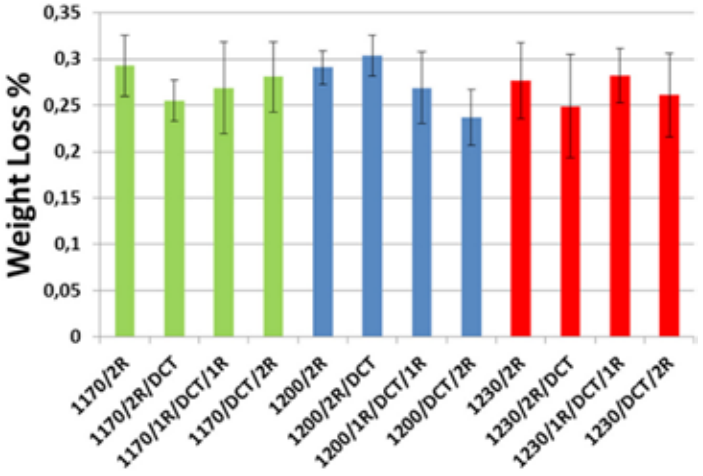

Figure 5: Weight loss after the abrasive wear test.

4 DISCUSSION

The results of HRC hardness tests are in agreement with those of other studies: DCT should not be applied after tempering. Yan and Li [19] report DCT should be performed before tempering because the martensite oversaturation attained at minus-196°C is associated with a higher nucleation rate and, therefore, results in a more homogeneous and finer carbide distribution. Molinari et al. [10] found better results for load-bearing steel when DCT was performed after the double tempering. However, this can be interpreted on the basis of higher toughness, which was relevant in the presence of the delamination.

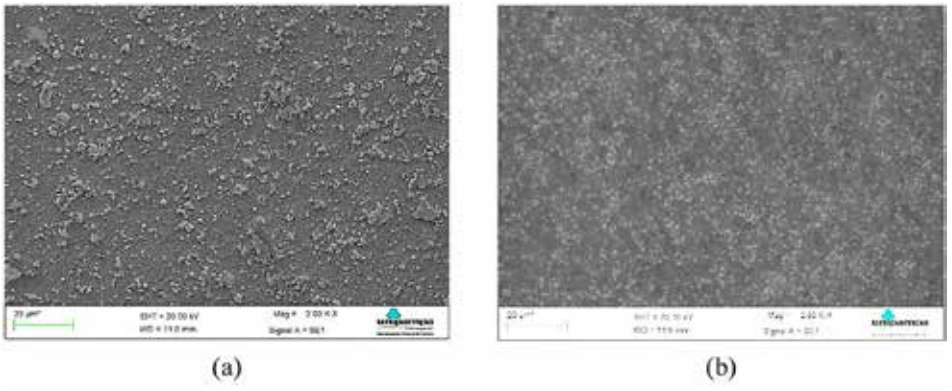

Figure 7: Carbide distribution for samples (a) 1170/2R and (b) 1170/DCT/2R.

Yan and Li [19] attributed the improvement in wear resistance by DCT to the matrix strengthening by fine secondary carbides and the formation of finer twinning. Mohan Lal et al. [12] concluded the mechanism causing the improvement in wear resistance is essentially an isothermal process, which cannot be explained then by austenite transformation. Additionally, Villa et al. [20] suggest that martensite formation at cryogenic temperature is partly time-dependent.

Li et al. [6] reported the amount of precipitated carbides in high-vanadium alloy steel subjected to DCT was three to five times greater than that observed in the samples exposed to conventional treatment. Das et al. [21] classify the carbides as primary carbides (PC), large secondary carbides (LSC) with a diameter from 0.5 to 2.0 μm, and small secondary carbides (SSC) with a diameter from 0.1 to 0.5 μm. They observed the population density of small secondary carbides (SSC) increases by 250% and doubles for large secondary carbides (LSC) after DCT. Furthermore, they reported a reduction of 34% in the mean diameter of SSC and 23% for LSC.

The values of the standard deviation of the hardness and microhardness measurements presented in Figure 4 and Table 3 suggest a greater homogeneity of the microstructure that are consistent with other studies, such as Koneshlou et al. [22] and Li et al. [23]. Furthermore, it is possible to observe that the amount of small carbides increases after DCT.

Bensely et al. [24] suggest the decrease in the temperature during cryogenic treatment increases the lattice defects and instability of the martensite, which drives the carbon and alloying elements to nearby defects. These clusters act as nuclei sites for the formation of fine carbides on subsequent tempering. The intensity of carbide precipitation depends on the extent to which the specimens are cooled.

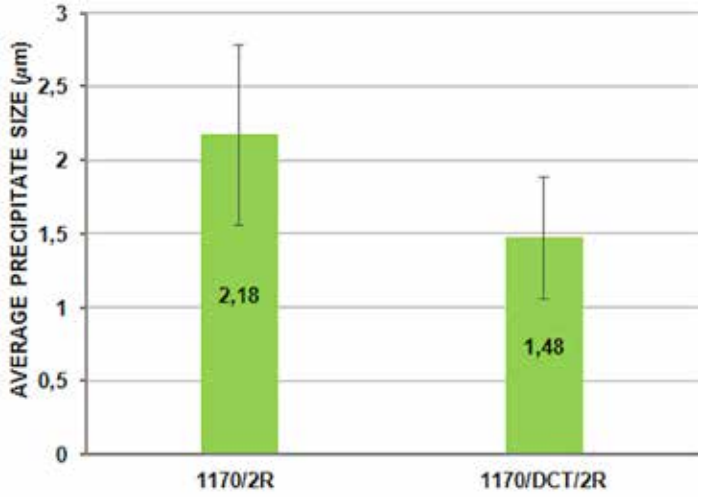

Figure 8: Effect of DCT on size and distribution of precipitates.

Tyshchenko et al. [25] suggest martensitic formation at low temperature is accompanied by plastic deformation of the virgin martensite due to the volume increase of the austenite-to-martensite transformation. Then, the plastic deformation of virgin martensite leads to an increase in the dislocation density and the capture and transport of immobile carbon atoms by moving dislocations and

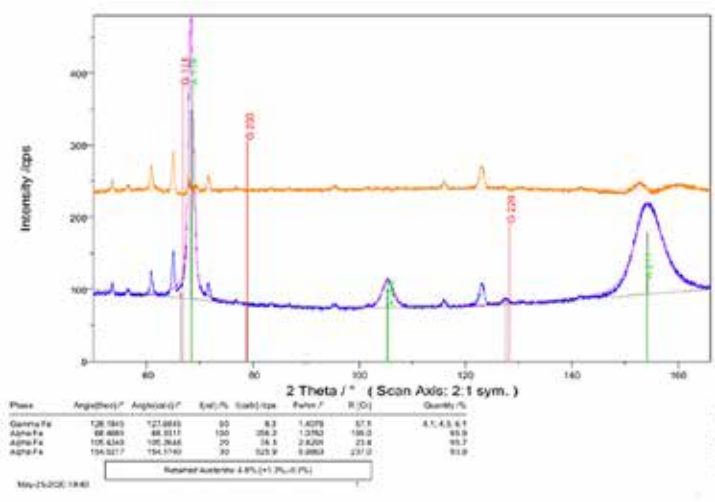

(a) Sample 1170/2R: 4.8% (+1.3,-0.7%)

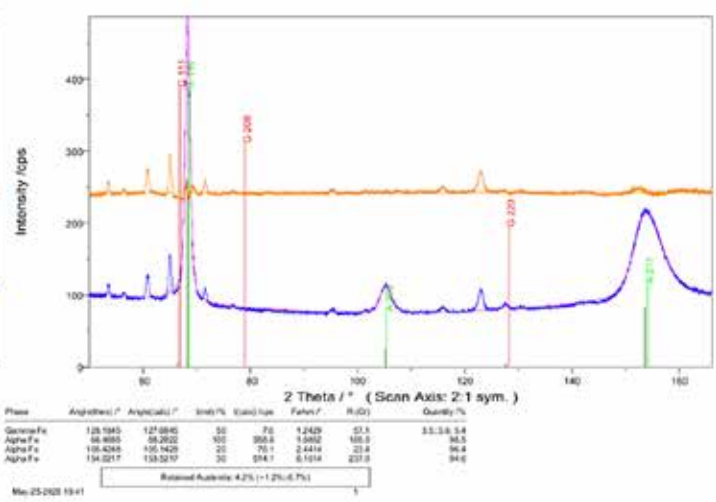

(b) Sample 1170/DCT/2R: 4.2% (+1.2,-0.7%)

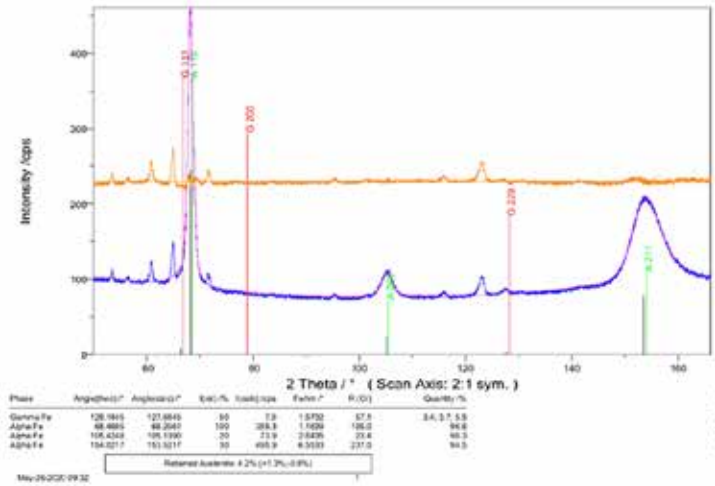

(c) Sample 1200/2R: 4.2% (+1.3,-0.8%)

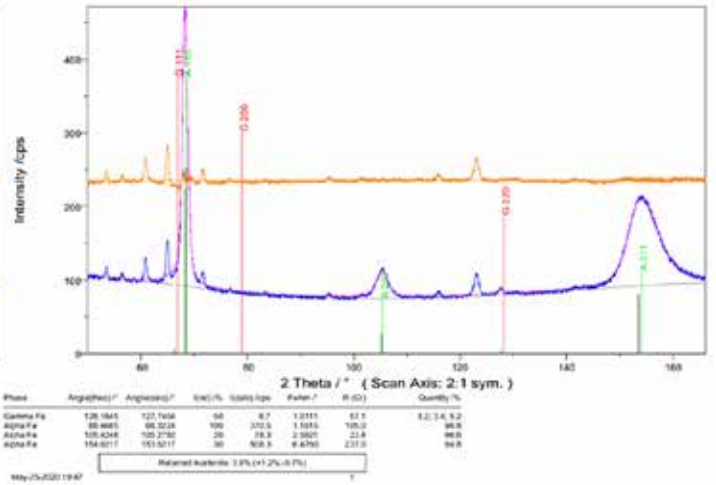

(d) Sample 1200/DCT/2R: 3.9% (+1.2, -0.7%)

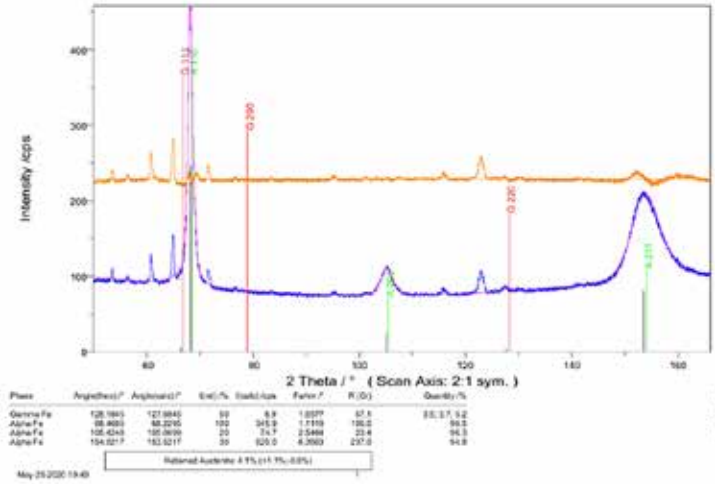

(e) Sample 1230/2R: 4.1% (+1.1, -0.6%)

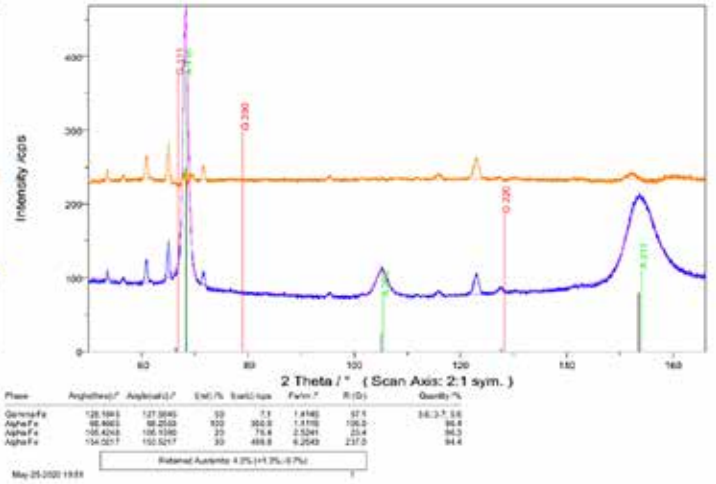

(f) Sample 1230/2R: 4.3% (+1.3,-0.7%)

Figure 6: Results from retained austenite measurements.

hence the formation of carbon clusters that can serve as sites for the nucleation of fine carbide particles during subsequent tempering. Therefore, Podgornik et al. [13] and Li et al. [6] proposed the reduced amount of carbon in the martensite, together with finer and more homogeneous carbide precipitation, provides improved fracture toughness. This is in agreement with the observations in this work that showed a reduction in size and in standard deviation of the carbide precipitations in the samples with DCT.

5 CONCLUSIONS

The present work indicates that cryogenic treatment should not be considered only as an add-on process to quenching and tempering but rather should be designed simultaneously. It is important to design all stages of heat treatment and deep cryogenic treatment (DCT) together because the results revealed the processes are interdependent. The following conclusions can be inferred:

» DCT applied after quenching and before tempering increases the hardness for AISI M2 steel and reduces the standard deviation of the hardness and microhardness measurements.

» The reduction of the standard deviation values of average hardness and average microhardness are associated with the greater homogenization of the carbides in the metal matrix.

» DCT increases the toughness of AISI M2 steel for austenitization temperature of 1,170 or 1,200°C.

» The best benefits observed for abrasive wear resistance are associated with the austenitization temperature of 1,200°C and DCT applied before double tempering.

» The best benefits observed for impact toughness are associated with the austenitization temperature of 1,170°C and DCT applied between double tempering.

» The level of retained austenite is the same after DCT.

» The improvement observed for impact toughness and abrasive wear resistance are associated with thinner scale precipitates and tougher martensite.

» For the heat-treatment routes investigated, DCT allows for the simultaneous increase in the toughness and wear resistance of the AISI M2 steel when proper heat and cryogenic treatments parameters are selected.

Sample	Average (J)	SD	Coefficient of variation	Increase compared with sample TEMP/2R
1170/2R	13.0	2.1	16%	–
1170/2R/DCT	17.5	0.7	4%	+35%
1170/1R/DCT/1R	20.3	1.8	9%	+56%
1170/DCT/2R	17.3	1.1	6%	+33%
1200/2R	14.3	1.8	12%	–
1200/2R/DCT	14.0	2.1	15%	-2%
1200/1R/DCT/1R	17.5	0.7	4%	+23%
1200/DCT/2R	18.8	0.4	2%	+32%
1230/2R 1	8.5	2.1	11%	–
1230/2R/DCT	15.8	0.4	2%	-15%
1230/1R/DCT/1R	15.0	0.7	5%	-19%
1230/DCT/2R	14.5	0.0	0%	-22%

Table 5: Results of the Charpy impact toughness test.

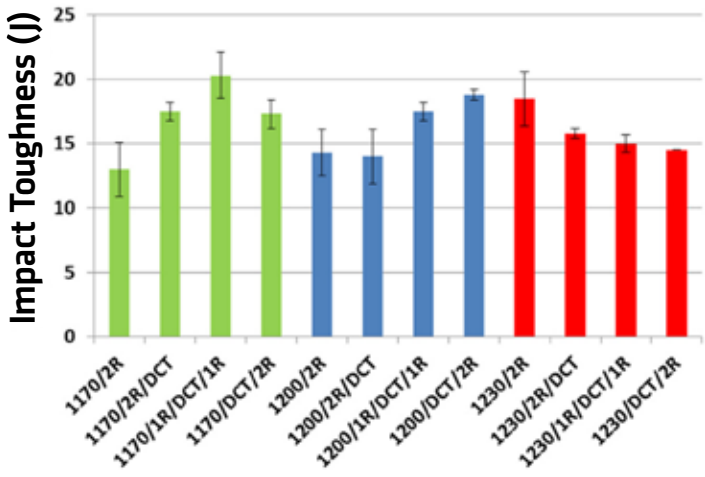

Figure 9: Impact toughness after Charpy test.

CONFLICTS OF INTEREST

The authors declare no conflicts of interest.

ACKNOWLEDGEMENTS

The authors thank the company Hurth Infer Indústria de Máquinas e Ferramentas Ltda. for performing the quenching treatment on the samples; the Universidade Regional Integrada – URI for the assistance with the Charpy test and FAPERGS-RS for the scholarship granted to the author C.T. Parcianello.

REFERENCES

[1] J.Y. Huang, Y.T. Zhu, X.Z. Liao, I.J. Beyerlein, M.A. Bourke, T.E. Mitchell; Microstructure of cryogenic treated M2 tool steel; Mater Sci Eng A, 339 (2003), pp. 241-244.

[2] F. Farhani, K.S. Niaki, S.E. Vahdat, A. Firozi; Study of the effects of deep cryotreatment on mechanical properties of 1.2542 tool steel; Mater Des, 42 (2012), pp. 279-288.

[3] P. Baldissera, C. Delprete; Deep cryogenic treatment: a bibliographic review; Open Mech Eng J, 2 (2008), pp. 1-11.

[4] V. Firouzdor, E. Nejati, F. Khomamizadeh; Effect of deep cryogenic treatment on wear resistance and tool life of M2 HSS drill; J Mater Process Technol, 206 (2008), pp. 467-472.

[5] F.J. Da Silva, S.D. Franco, A.R. Machado, E.O. Ezugwu, A.M. Souza Jr.; Performance of cryogenically treated HSS tools; Wear, 261 (2006), pp. 674-685.

[6] H. Li, W. Tong, J. Cui, H. Zhang, L. Chen, L. Zuo; The influence of deep cryogenic treatment on the properties of high-vanadium alloy steel; Mater Sci Eng A, 662 (2016), pp. 356-362.

[7] K. Amini, A. Akhbarizadeh, S. Javadpour ; Investigating the effect of holding duration on the microstructure of 1.2080 tool steel during the deep cryogenic heat treatment; Vacuum, 86 (2012), pp. 1534-1540.

[8] A. Akhbarizadeh, S. Javadpour; Investigating the effect of as-quenched vacancies in the final microstructure of 1.2080 tool steel during the deep cryogenic heat treatment; Mater Lett, 9 (2013), pp. 247-250.

[9] J.D. Darwin, D. Mohan Lal, G. Nagarajan; Optimization of cryogenic treatment to maximize the wear resistance of chrome silicon spring steel by Taguchi method; Int J Mater Sci, 2 (1) (2007), pp. 17-28.

[10] A. Molinari, M. Pellizzari, S. Gialanella, G. Straffelini, K.H. Stiasny; Effect of deep cryogenic treatment on the mechanical properties of tool steel; J Mater Process Technol, 118 (2001), pp. 350-355.

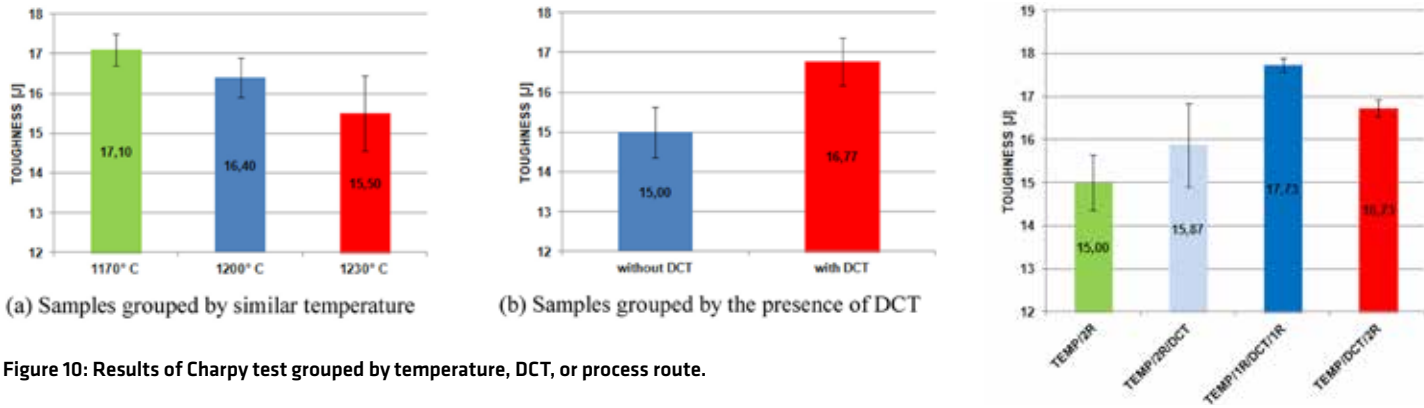

Figure 10: Results of Charpy test grouped by temperature, DCT, or process route.

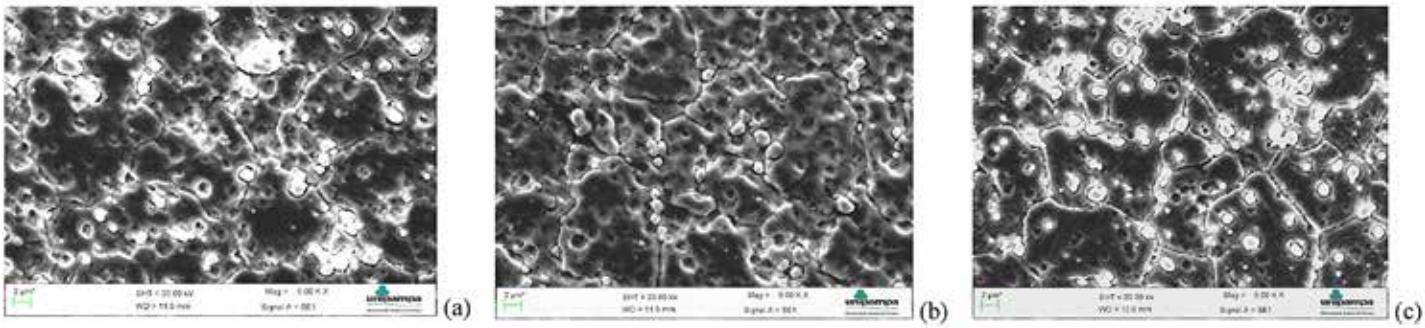

Figure 11: Grain size after austenitizing at (a) 1,170 °C, (b) 1,200 °C, and (c) 1,230 °C.

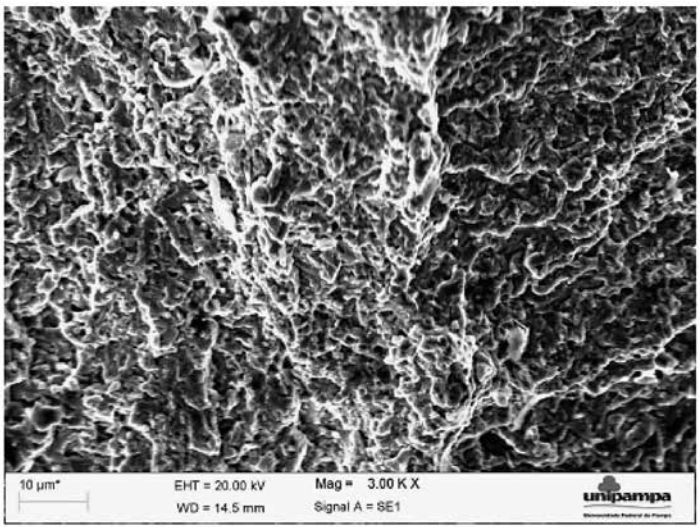

Figure 12: Fracture observed by SEM at 3,000× for sample 1200/DCT/2R.

[11] D. Senthilkumar, I. Rajendran; A research review on deep cryogenic treatment of steels; Int J Mater Struct Integrity, 8 (1/2/3) (2014), pp. 169-184.

[12] D. Mohan Lal, S. Renganarayanan, A. Kalanidhi; Cryogenic treatment to augment wear resistance of tool and die steel; Cryogenics, 41 (2001), pp. 149-155.

[13] B. Podgornik, I. Paulin, B. Zajec, S. Jacobson, V. Lesvovsek; Deep cryogenic treatment of tool steels; J Mater Process Technol, 229 (2016), pp. 398-406.

[14] D. Das, A.K. Dutta, K.K. Ray; Inconsistent wear behaviour of cryotreated tool steel: role of mode and mechanism; Mater Sci Technol-Lond, 25 (10) (2009), pp. 1249-1257.

[15] A. Akhbarizadeh, A. Shafyei, M.A. Golozar; Effects of cryogenic treatment on wear behavior of D6 tool steel; Mater Des, 30 (2009), pp. 3259-3264.

[16] N.S. Kalsi, R. Sehgal, V.S. Sharma; Cryogenic treatment of tool materials: a review;Mater Manuf Process, 25 (2010), pp. 1077-1100.

[17] E.R. Morgan, T. Ko; Thermal stabilization of austenite in iron-carbon_nickel alloys; Acta Metall, 1 (1953), pp. 36-48.

[18] O.N. Mohanty; On the stabilization of retained austenite: mechanism and kinetics; Mater Sci Eng B, 32 (1995), pp. 267-278.

[19] X.G. Yan, D.Y. Li; Effects of sub-zero treatment condition on microstructure, mechanical behavior and wear resistance of W9Mo3Cr4V high speed steel; Wear, 302 (2013), pp. 854-862.

[20] M. Villa, M.F. Hansen, M.A.J. Somers; Martensitic formation in Fe-C alloys at cryogenic temperatures; Scr Mater, 141 (2017), pp. 129-132.

[21] D. Das, A.K. Dutta, K.K. Ray; Influence of varied cryotreatment on wear behavior of AISI D2 Steel Wear, 266 (2009), pp. 297-309.

[22] M. Koneshlou, K. Kaveh Meshinchi Asl, K. Farzad; Effect of cryogenic treatment on microstructure, mechanical and wear behaviors of AISI H13 hot work tool steel; Cryogenics, 51 (2011), pp. 55-61.

[23] J. Li, X. Yan, X. Liang, H. Guo, D.Y. Li; Influence of different cryogenic treatments on high-temperature wear behavior of M2 steel; Wear, 376-377 (2017), pp. 1112-1121.

[24] A. Bensely, S. Venkatesh, D. Mohan Lal, G. Nagarajan, A. Rajadurai, J. Krzysztof; Effect of cryogenic treatment on distribution of residual stress in case carburized En 353 steel; Mater Sci Eng A, 479 (2008), pp. 229-235

[25] A.I. Tyshchenko, W. Theisen, A. Oppenkowski, S. Siebert, O.N. Razumov, A.P. Skoblik, et al.; Low-temperature martensitic transformation and deep cryogenic treatment of a tool steel; Mater Sci Eng A, 527 (2010), pp. 7027-7039.

ABOUT THE AUTHORS

Dieison G.Fantineli, Cleber T.Parcianello, Tonilson S.Rosendo, and Marco D.Tier are with the Universidade Federal do Pampa – PPEng/UNIPAMPA, Alegrete, RS, Brazil. Afonso Reguly is with the Universidade Federal do Rio Grande do Sul – LAMEF/PPGE3M/UFRGS, Porto Alegre, Brazil.

VACUUM HEAT TREATING AND ALUMINUM ALLOYS

Investigating the effect of vacuum heat treatment on microstructures and the mechanical properties of 7A52 aluminum alloy-Al_2O_3 ceramic brazed joints

By DEKU ZHANG, XUSHENG QIAN, XIAOPENG LI, and KEHONG WANG

This study investigated the interface morphology, microstructure composition, and connection strength of 7A52 aluminum alloy-Al_2O_3 ceramic brazed joints under heat-treatment conditions. Alumina ceramics were first treated with electroless nickel plating, followed by vacuum heat treatment at different temperatures. Then, an Al-Si-Mg intermediate layer was placed between the treated alumina ceramic and 7A52 aluminum alloy for brazing under the conditions of welding temperature 590, holding time 1 hour, pressure 2 MPa. Results showed that when heat treatment was performed at 350°C and below, the nickel-plated metal had an amorphous structure, and when performed at 400°C, the nickel-plated layer had a crystalline structure and the brittle phase Ni_3P was precipitated. When the heat-treatment temperature was 350°C, the joint shear strength reached the maximum, which was 68.7 MPa.

INTRODUCTION

Aluminum alloy has been widely used in structural parts of airplanes, rockets, ships, and lightweight vehicles for its excellent mechanical properties and high-specific strength. Among them, 7A52 aluminum alloy has the advantages of high-specific strength, high-specific rigidity, and strong heat resistance, making it widely used in reducing weight for the automobile industry [Feng et al., 2016]. However, as society has developed, the number of vehicles on the road has grown rapidly, making the road safety situation increasingly complex. Therefore, as road vehicles, especially special vehicles, become more lightweight, it is necessary to improve the vehicle protection performance as much as possible.

Ceramics have high hardness, high compressive strength, and good elastic properties, but its brittleness limits the application. Combining it with aluminum alloy, which has high-specific strength and low density, high-performance lightweight composite materials can be manufactured, which can greatly reduce the weight of the auto bodies. However, in the manufacturing process of ceramic-metal composite materials, there exists a problem of reliable connection between metal aluminum alloy and alumina ceramic with different physical and chemical properties [Gama et al., 2001; Tasdemirci et al., 2012; Serjouei et al., 2017]. At present, there are more methods for metal sealing ceramic, each with its own advantages, disadvantages, and limitations. Currently, commonly used ballistic ceramics mainly include Al_2O_3, SiC, Si_3N_4, B_4C, etc. Existing research results show the connection of aluminum and ceramic has a great influence on auto bodies' performance.

At present, many methods of connecting alumina ceramic and aluminum have been developed, such as diffusion bonding, friction bonding, active casting, active surface crimping, electrostatic pressure bonding, ultrasonic welding, indirect brazing, etc. For example, Nicholas and Crispin realized the connection of aluminum and alumina ceramic in argon or vacuum with a pressure of 50 MPa and a connection time of 30 minutes [Nicholas and Crispin, 1982]. Fauzi et al. used the friction connection method to realize the connection between alumina ceramic and aluminum under the conditions of rotation speed 1,250–2,500 rpm, pressure 7 Mpa, and pressure time 20 seconds [Ahmad Fauzi et al., 2010]. Peng Rong et al. used the active casting method to manufacture Al-Al_2O_3 ceramic joint samples at 660-750°C and measured the tensile strength of the connection interface [Peng et al., 2002]. TWI enterprise manufactured composite products of alumina ceramic and aluminum made by ultrasonic welding.

Since the oxide film on the aluminum surface hinders the wetting of aluminum and ceramic, the interface residual stress is high. The joint strength of the above method is generally not high, and it is easy to cause cracking. In order to improve the wettability, relieve residual stress, increase the strength, and inhibit cracking, in addition to the pre-treatment of aluminum alloy before welding, indirect brazing can be used, such as plating Ni on the ceramic surface and then brazing with aluminum-based solder. Nickel-based amorphous materials prepared by electroless plating often show high catalytic activity in the field of catalysis. At the same time, it is often used in the preparation of anti-corrosion materials. The anti-corrosion film is plated on the metal surface without electricity to achieve the same effect as electroplating [Song et al., 2020]. Since the amorphous plating is a high-energy state and has internal stress, it still has a certain impact on the joint performance. After heat treatment of the plated parts, the internal stress in the plating relaxes as the microscopic defects of the crystal lattice are eliminated.

Element	Si	Fe	Cu	Mn	Mg	Cr	Zn	Ti	Al
wt%	0.25	0.35	0.05–0.2	0.2–0.5	2.0–2.8	0.15–0.25	4.0–4.8	0.18	Bal

Table 1: Main chemical composition of 7A52 aluminum alloy.

In this article, electroless nickel plating was performed on the alumina ceramic surface, and the nickel-plated ceramics were heat treated. An Al-Si-Mg intermediate layer was placed between the alumina ceramic and 7A52 aluminum alloy for brazing. The interface morphology, microstructure composition, and connection strength of 7A52 aluminum alloy-Al_2O_3 ceramic brazed joints under heat treatment conditions were investigated.

MATERIALS AND METHODS

The aluminum alloy used for research was 7A52 aluminum alloy, which had been widely used as a composite armor material in engineering. The main chemical composition of the alloy is shown in Table 1. Before welding, it is necessary to remove impurities and oxide film on the aluminum alloy surface. First, degrease the surface with acetone solvent, then alkali wash with 10% NaOH solution at 50°C for 5 minutes, and then rinse with running water. After alkaline washing, acid wash with 30% HNO_3 solution at 60°C for 2 minutes,

then rinse with running water, and, finally, dry at low temperature.

The pressure brazing was carried out under the conditions of welding temperature 590°C, holding time 1 hour, pressure 2 MPa by vacuum hot pressing brazing furnace, and the vacuum degree of the vacuum furnace was 1.33×10^{-3}Pa. The Al_2O_3 ceramic ball used in the experiment, whose diameter was 10 mm, was treated with surface electroless Ni-P plating. The main process of electroless nickel plating in this article was: pretreatment → degreasing → coarsening → sensitization → activation → reduction → plating. The size of 7A52 aluminum alloy was $16 \times 16 \times 8$ mm^3, and the thickness of Al-Si-Mg solder was 0.1 mm. The three were assembled in order, and the assembly diagram was shown in Figure 1. Before the experiment, Al-Si-Mg filling material was cut into a square with 18 mm side length, and then washed with 15% hot sodium hydroxide solution (50°C) for 30-40 seconds, rinsed immediately with running water after the alkaline washing. Then it was washed with 10% nitric acid solution for 10-15 seconds, rinsed with running water shortly after washing and finally placed between the samples.

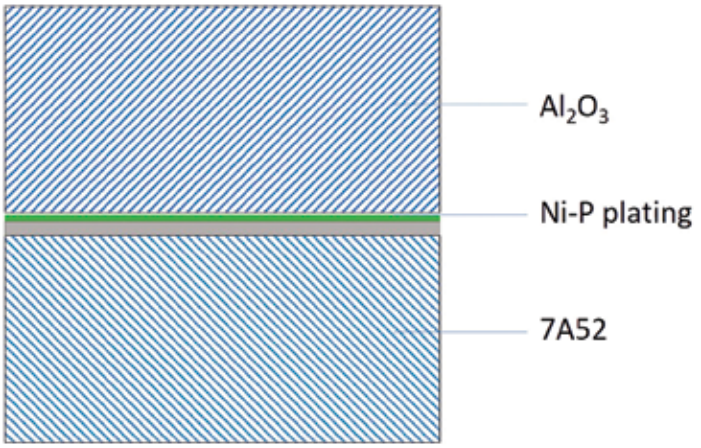

Figure 1: Assembly structure schematic.

RESULTS AND DISCUSSION

Evolution of Ceramic Surface Plating

The physical and chemical properties of Al_2O_3 ceramic and 7A52 aluminum alloy were different. In order to improve the poor wettability and low bonding strength of ceramic and metals, the method of electroless nickel plating was used to realize the metallization of ceramic surface. Studies showed the Ni-P plating crystalline structure obtained by electroless plating had three types. In general, when the phosphorus content in the plating was less than 3%, the plating structure was crystalline; when the phosphorus content was greater than 8%, the plating structure was amorphous; when the phosphorus content was 3% to 8%, the plating structure was the mixture of non-crystals and microcrystals. In this experiment, the phosphorus content in the plating was about 8.5% [Zou et al., 2004]. The amorphous plating was in a high-energy state and had internal stress; the internal stress would be relaxed to a certain extent after plating heat treatment. If the heat-treatment temperature was higher than the crystallization temperature, the amorphous structure would first be transformed into crystallites, and then the crystallites would further grow into grains [Li et al., 2015]. In addition, high-vacuum heat-treatment process can also release the hydrogen adsorbed in the plating during electroless plating to a certain extent. Therefore, when the vacuum heat-treatment temperature was low, as the heat-treatment temperature rose, the bonding strength between the plating and the substrate increased. However, when the heat-treatment temperature rose further, on the one hand, the grains would be further coarsened, and brittle phases such as Ni_3P would be precipitated on the Ni-P plating. On the other hand, due to the difference in the athermal expansion coefficient between the substrate and the plating, a new residual stress would be formed while the internal stress generated by the state tissue relaxed in the amorphous. Therefore, if the heat-treatment temperature was too high, it would lead to the plating cohesion, and the bonding strength of plating and substrate decrease [Zhang et al., 2004].

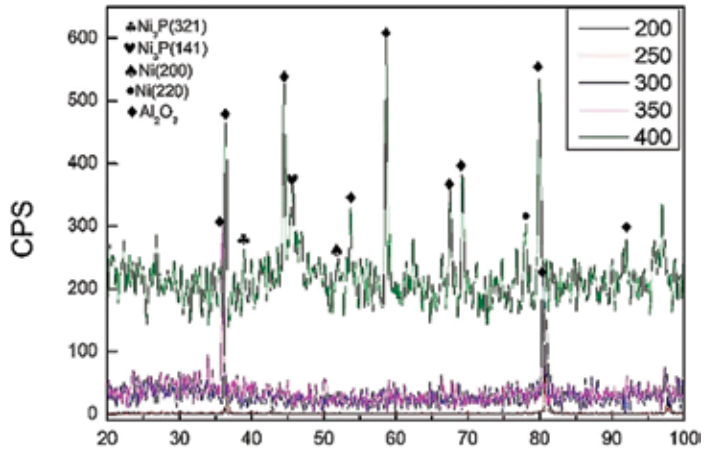

Figure 2: X-ray diffraction analysis results.

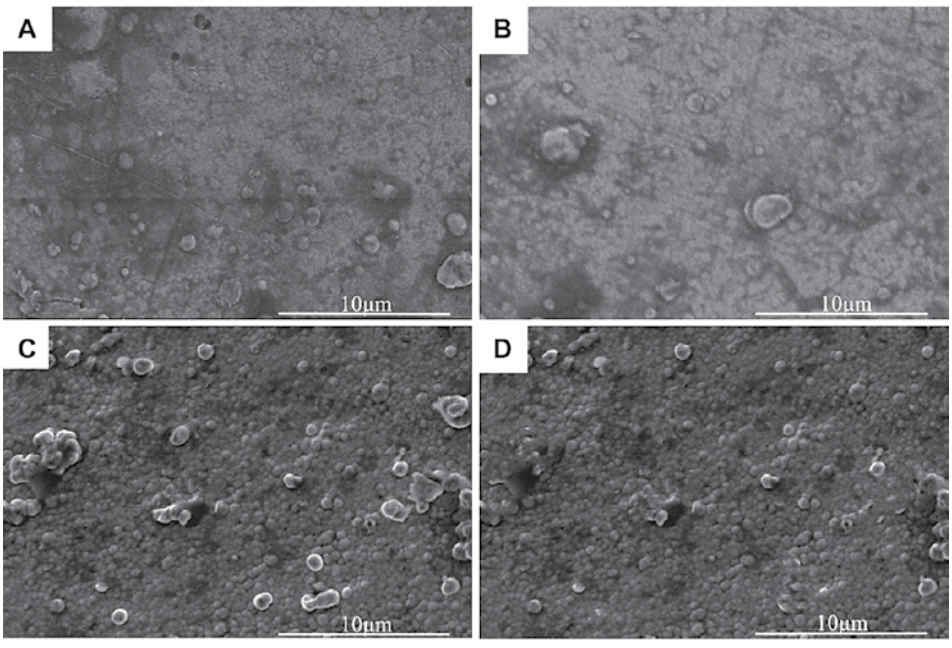

Figure 3: Micromorphology of the nickel-plated layers after 1 hour heat treatment at different temperatures: (A) 200°C, (B) 250°C, (C) 300°C, (D) 350°C.

When performing vacuum heat treatment on nickel-plated ceramic, the vacuum degree was 5×10^{-3} Pa, the holding time was 1 hour, and the heat-treatment temperature was 200, 250, 300, 350, and

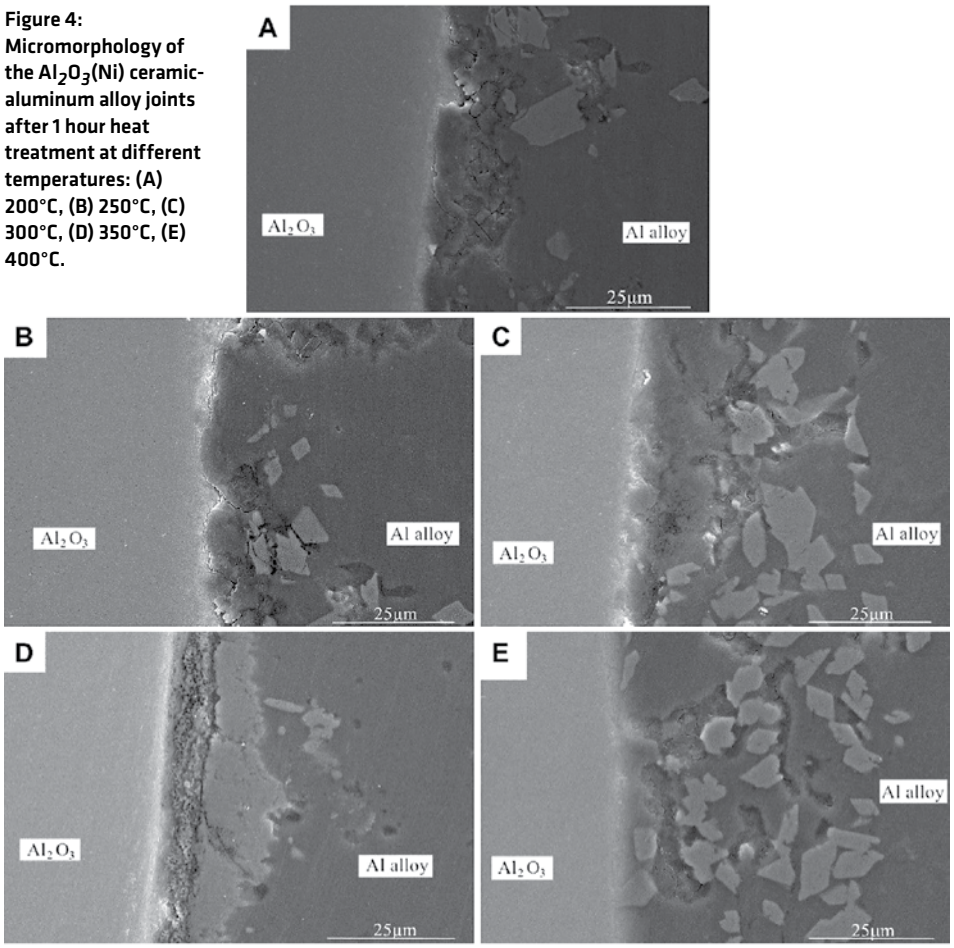

Figure 4: Micromorphology of the Al_2O_3(Ni) ceramic-aluminum alloy joints after 1 hour heat treatment at different temperatures: (A) 200°C, (B) 250°C, (C) 300°C, (D) 350°C, (E) 400°C.

400°C. Figure 2 shows the X-ray diffraction analysis results of the nickel-plated layer on the ceramic surface after vacuum heat treatment.

In Figure 2, when the temperature was below 350°C, the diffraction peaks of Ni and P related crystalline structure were not seen in the plating. When the temperature was kept at 400°C for 1 hour, the diffraction peaks of Ni and Ni_3P appeared, indicating that a certain amount of crystalline structure appeared at this time. Ni_3P and other crystalline structures were brittle phases, which was not conducive to improving the welded joint strength of aluminum alloy and ceramic.

Figure 3 showed the micromorphology of the nickel-plated layers on the Al_2O_3 surface after heat treatment at different temperatures. In Figure 3, after vacuum heat treatment, bubble-like spherical clusters were generated on the nickel-plated layer surface, and the diameter of the spherical clusters was about 1-2 μm. As shown in Figure 3A, when the heat-treatment temperature was 200°C, there were only a few clusters on the plating surface. And as shown in Figure 3B, C, D, with the increase of the vacuum heat-treatment temperature, the spherical clusters grew in number and became denser. This was because hydrogen was generated during the electroless nickel plating process. The hydrogen existed inside the plating. At the same time, there are defects and internal stress in the plating. When the heat-treatment temperature was 200°C, the residual hydrogen in the plating escaped, eliminating the defects and internal stress. Due to the low heat-treatment temperature at this time, little hydrogen was released, so there were not many clusters on the plating surface. However, as the heat-treatment temperature rose, more hydrogen inside the plating escaped, so the spherical clusters on the surface of the plating became denser. At the same time, the defects and internal stress of the plating were eliminated more fully.

The Interface of 7A52 Aluminum Alloy-Al_2O_3 Ceramic Hot-Press Diffusion Brazing Joints

In order to effectively improve the bonding performance of 7A52 aluminum alloy and Al_2O_3 (Ni) ceramic, improve the connection process between the two, and increase the joint strength, after vacuum heat treatment of the nickel-plated Al_2O_3 ceramic, the Al-Si-Mg intermediate layer was subjected to hot press diffusion to realize the welding of the two. Figure 4 shows the micromorphology of Al_2O_3(Ni) ceramic-aluminum alloy joints at different heat treatment temperatures when the process conditions were 590°C, 2 MPa, and 1 hour.

It can be seen from Figure 4 that, after vacuum heat treatment, there were no gaps, cracks, holes, or other defects at the interface between the nickel-plated metal layer and the Al_2O_3 ceramic. Compared with the interface without heat treatment, it had a tighter combination and a more natural transition. As shown in Figure 4A-E, with the rise of the heat-treatment temperature, the interface became more natural and the combination became tighter. When the heat treatment increased to 400°C, there was no interface between the nickel-plated metal layer and the aluminum alloy. This

is because that, after vacuum heat treatment, the internal defects and internal stress of the nickel-plated layer were eliminated, and as the heat treatment temperature rose, the layer structure became denser. Besides, during the welding process, the solid Ni continually diffused into the Al-Si-Mg and reacted with Al to form an Al-Ni intermetallic compound. It can also be seen from Figure 4 that many irregular blocky substances were scattered at the interface between the intermediate layer and the aluminum alloy. It was speculated that they were formed by the crushing of the nickel-plated layer under pressure, and their composition was an Al-Ni intermetallic compound.

The above micromorphology analysis revealed the 7A52 aluminum alloy was tightly combined with the vacuum heat-treated Al_2O_3 (Ni) ceramic, the joints had natural transition,s and no defect. In order to explore the distribution status and changing trend of interface elements, EDS was used to scan the joints by line scan and point scan. Figure 5 show the EDS scanning analysis spectra of the joints' elements under different heat-treatment temperatures. It can be seen from Figure 4 that the micromorphology of the nickel plating on the ceramic surface under 200°C heat treatment was relatively similar to it under 250°C, and that under 300°C was similar to 350°C, so it just analyzed the line scan of the joints under 250, 300, and 400°C.

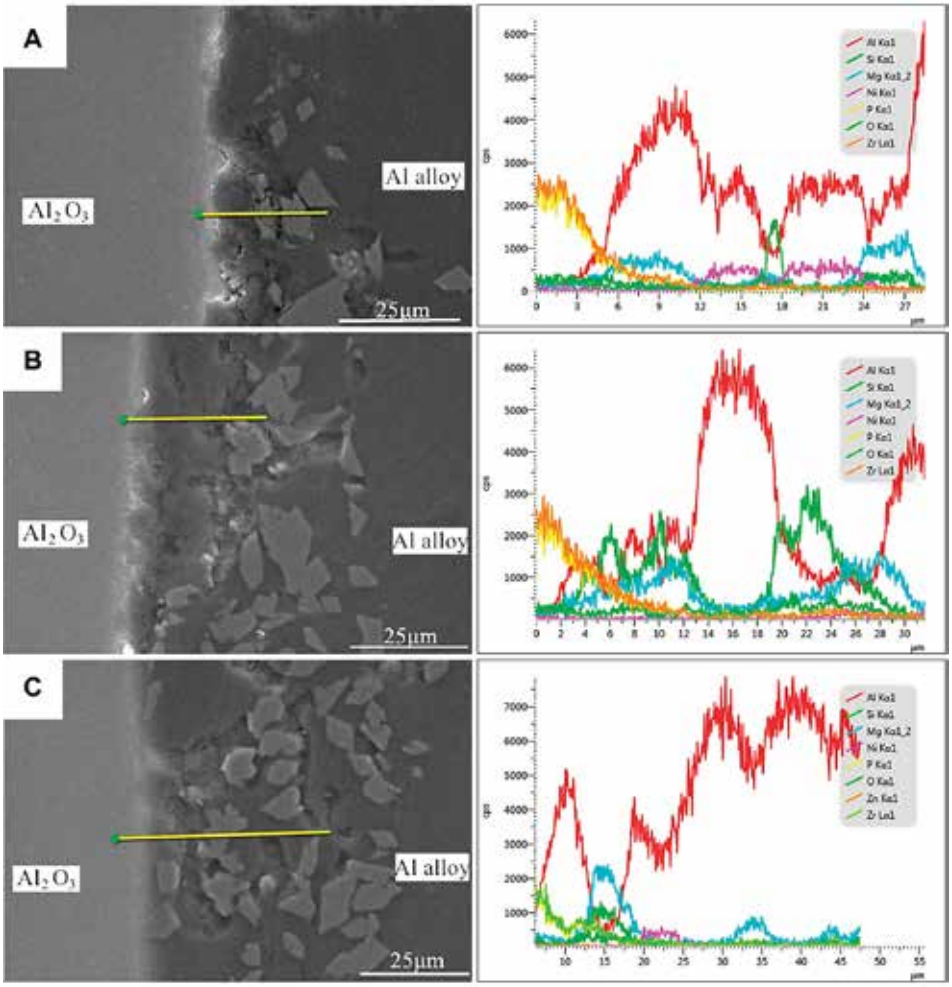

Figure 5: EDS line scan results of the Al_2O_3(Ni) ceramic-aluminum alloy joints after 1 hour heat treatment at different temperatures: (A) 250°C, (B) 300°C, (C) 400°C.

In Figure 5A, the Al element content was the highest. From the scan line starting point to 10 μm, the Al element content increased greatly, and the Mg element also increased, while the Ni element with low content changed little. Therefore, this range was the Al-Si-Mg solder zone. At the scan line 10-12 μm, the Al element content decreased relatively, while the Ni element content showed an increasing trend, so this range was the junction of the solder and the nickel-plated metal layer. At the scan line 12-16 μm, the element contents of Al and Ni were relatively high at the same time. In this range, the nickel-plated layer reacted with the Al element, which generated many Al-Ni intermetallic compounds, making the element contents of Al and Ni high. Thus, this range was the Al-Ni intermetallic compounds zone. At the scan line 16-18 μm, the element contents of Al and Ni decreased, but the Si element content increased sharply. This was due to the formation of an Al-Si eutectic phase. At the scan line 18-24 μm, the elements change similarly to that at 12-16 μm, which would not be repeated here. At the scan line 24-27 μm, Al, Si, and Mg elements all showed an increasing trend, and, at the same time, the Ni element content decreased to the lowest. This range was considered to be the Al-Si-Mg solder zone. It is worth noting that the Zr element content gradually decreased from the scan line starting point to 10 μm, and then the content had been stable at a very low level. In this experiment, only the 7A52 aluminum alloy contained Zr, thus it can be known that the active element Zr in the aluminum alloy diffused, gathered on the Al_2O_3 ceramic surface and reacted with it.

In Figure 5B, the element contents of Al, Si, and Mg were all at a relatively high level at the scan line 4-14 μm and 20-28 μm. Therefore, it can be seen that this range was the solder zone. At scan line 14-20 μm, the Al element content was the highest, and the other elements' contents were at the lowest level. It was considered that Si and Mg in this range diffused to both sides, thus forming peaks of Mg and Si on both sides. Now that Mg and Si had the lowest element contents here, Al had the highest. In addition, the Zr element was similar to that shown in Figure 5A, which gathered on the Al_2O_3 ceramic surface.

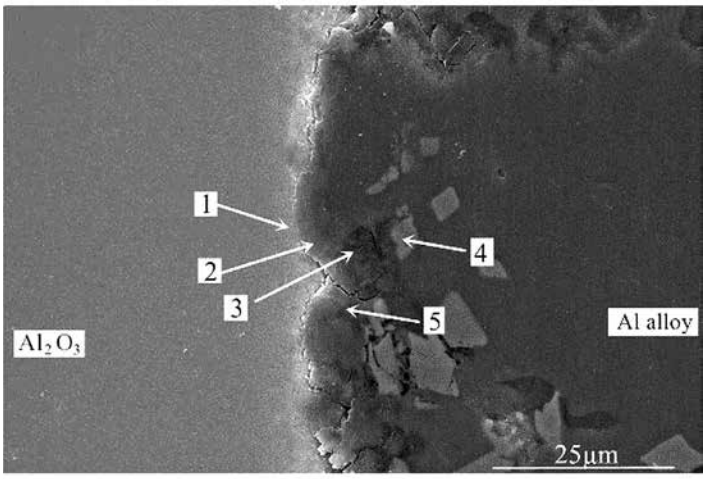

Figure 6: EDS point scan of the Al_2O_3(Ni) ceramic-aluminum alloy joint after 1 hour heat treatment at 250°C.

In Figure 5C, at the scan line 10-20 μm, the element contents of Si and Mg were at relatively high levels, and the Al element content

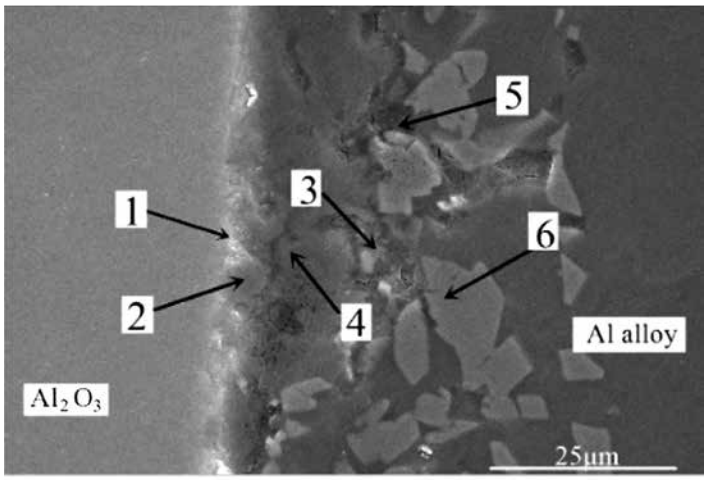

Figure 7: EDS point scan of the Al_2O_3(Ni) ceramic-aluminum alloy joint after 1 hour heat treatment at 300°C.

Location	Al	O	Mg	Si	Ni	P	Phase
1	34.95	62.93	0.87	1.04	0.2	0	Al_2O_3
2	26.54	53.11	13.27	1.17	0.1	5.81	$MgAl_2O_4$
3	70.78	4.36	7.71	10.22	0.09	6.84	Al-Si-Mg solder
4	66.93	2.61	8.92	1.31	16.84	3.39	Al_3Ni
5	68.54	3.26	10.51	11.24	1.13	5.32	Al-Si-Mg solder

Table 2: EDS scan results of each point in Figure 6 (at%).

Location	Al	O	Mg	Si	Ni	P	Zr	Phase
1	11.9	64.07	2.87	0.78	0.14	2.05	18.19	ZrO_2、Al_2O_3
2	16.28	56.21	8.14	1.42	0.2	5.94	11.81	ZrO_2、$MgAl_2O_4$
3	38.45	0.38	28.24	27.61	2.99	2.33	0	Al-Si-Mg solder
4	49.15	0.38	15.73	32.35	0.84	1.55	0	Al-Si-Mg solder
5	49.80	1.86	21.39	22.34	0.92	3.68	0	Al-Si-Mg solder
6	74.46	1.59	2.20	1.02	20.71	0.03	0	Al_3Ni

Table 3: EDS scan results of each point in Figure 7 (at%).

was relatively low. It was considered that this range was the solder zone. The Mg element in the solder gathered here, making the Mg element content the highest. At the scan line 20-25 μm, the Al element content was high, and the Ni element content was the highest. According to the previous analysis, it can be seen that there were many Al-Ni intermetallic compounds in this range.

From Al_2O_3 ceramic to aluminum alloy, according to the above analysis, the following zones existed at the joint interface: Zr-ceramic reaction zone, solder zone, Al-Ni intermetallic compound zone, and Al-Si eutectic zone. In addition, the solder zone, Al-Ni intermetallic compound zone, and Al-Si eutectic zone were intertwined.

In order to accurately analyze the elemental composition at the interface between the vacuum heat-treated Al_2O_3(Ni) ceramic and the 7A52 aluminum alloy, an EDS point scan was performed. Figure 6 shows the selected points at the interface of the joint under 250°C heat treatment. Table 2 show the corresponding composition of each point in Figure 6. Figure 7 shows the selected points at the interface of the joint under 300°C heat treatment. Table 3 shows the corresponding components at each point in Figure 7.

In Table 2, at position 1, the main composition was Al_2O_3, and the Mg and Si elements diffused to there. At position 2, the main component was spinel. It was considered that the liquid phase was generated after the solder reached the eutectic temperature, then the active element Mg in the solder diffused and gathered to this point and reacted with the Al_2O_3 ceramic. The reaction product was spinel, an enhanced phase in the interface. At position 3, it was the Al-Si-Mg filling material zone, where the Al element content was high. At position 4, the main composition was Al3Ni intermetallic compound, which was the result of the interaction between the filling material and the nickel-plated layer. Position 5 was the same as position 3, which was the Al-Si-Mg solder zone. According to the above analysis, the structures at the joint interface were: Al_2O_3 ceramic/spinel ($MgAl_2O_4$)/Al-Si-Mg brazing filler metal zone/Al_3Ni/7A52 aluminum alloy.

In Table 3, the Zr element appears at position 1. In this experiment, only the 7A52 aluminum alloy contained Zr. Zr was an active element and had a high affinity for O element. The Zr element diffused from the aluminum alloy and gathered at position 1, and then reacted with O element to generate ZrO_2. Since the Zr element content in 7A52 aluminum alloy was only 0.05-0.15%, it was certain that ZrO_2 generated at the interface was very small. There was also Al_2O_3 in position 1. ZrO_2 also appeared at position 2, and the active element Mg in the solder reacted with the Al_2O_3 ceramic to generate a spinel ($MgAl_2O_4$) reinforcing phase. Positions 3, 4, and 5 were located outside of the reaction zone of the solder and ceramic (the spinel generation zone), so here was the brazing filler metal zone. At position 6, the Al_3Ni intermetallic compound was inferred to be generated based on the atomic percentage, which corroborated the previous analysis. The filling material reacted with solid Ni, continuously dissolving the nickel-plated metal layer; meanwhile, a certain pressure was applied during the welding process. Under the combined action of the two, the morphology of the nickel-plated layer became fragmented, and Al-Ni intermetallic compounds were formed in the layer. Therefore, under this process condition, the interface structures of the joint were: Al_2O_3 ceramic/ZrO_2 (trace amount)/spinel ($MgAl_2O_4$)/Al-Si-Mg brazing filler metal zone/Al_3Ni/7A52 aluminum alloy.

After 400°C heat treatment, the interface structure of Al_2O_3(Ni) ceramic-7A52 aluminum alloy joint was the same as that of 300°C.

Strength Analysis of 7A52 Aluminum Alloy-Al_2O_3 Ceramic Hot-Press Diffusion Brazing Joints

Figure 8 shows the shear strength of 7A52 aluminum alloy-Al_2O_3(Ni) ceramic pressure brazed joints under the conditions of welding temperature 590°C, holding time 1 hour, pressure 2 MPa, and different heat-treatment temperatures. It can be seen from Figure 8 that the joint had the lowest strength, 38 MPa, when the vacuum heat-treatment temperature was 200°C. Without heat treatment, under the same welding process conditions, the joint strength was 19.8 MPa. Therefore, the heat-treatment process had a significant effect on the improvement of joint strength. It was analyzed that, due to

the electroless plating implemented in this experiment, the P element content w(P) on the surface of the Ni-P metal layer was 8.5%, so the plating metal was amorphous. The amorphous plating was in a high-energy state and had internal stress; the internal stress would be relaxed to a certain extent after plating heat treatment. And the H element adsorbed in the plating during the plating process could be released to a certain extent. Therefore, the bonding strength of the plating and the ceramic would be somewhat improved, the "locking" effect became stronger, and the combination became tighter, which had a significant effect on improving the strength of the brazed joints. Besides, as the vacuum heat-treatment temperature increased, the joint strength gradually increased. When the temperature rose to 350°C, the joint strength reached the maximum, which was 68.7 MPa. This was because the higher the heat-treatment temperature, the better the relaxation of internal stress and the release of H elements in the plating. Thus, the bonding strength between the plating and the substrate gradually increased, and then the strength of the brazed joint also gradually increased. However, when the heat-treatment temperature increased from 350 to 400°C, the joint strength decreased from 68.7 to 50.18 MPa, decreased by 27%. It was analyzed that 400°C was higher than the crystallization temperature of the nickel-plated layer. The nickel-plated layer first transformed from an amorphous structure to microcrystalline, and then the microcrystals grew further. There was a difference in the thermal-expansion coefficient between the nickel-plated layer and the Al_2O_3 ceramic. Excessive heat-treatment temperature imposed the nickel-plated layer to generate new residual stress, which made the bonding effect of the layer and the Al_2O_3 ceramic matrix worse. Therefore, the strength of the brazed joint decreased. Meanwhile, according to the X-ray diffraction results, Ni_3P(321) and Ni_3P(141) were precipitated on the surface of the nickel-plated layer when the heat-treatment temperature was 400°C. The two precipitated substances were both brittle phases, making the nickel-plated layer more vulnerable to crushing under pressure and then decreasing the bonding strength of the layer and the Al_2O_3 ceramic matrix, which was also the reason for the decrease of brazed joint strength.

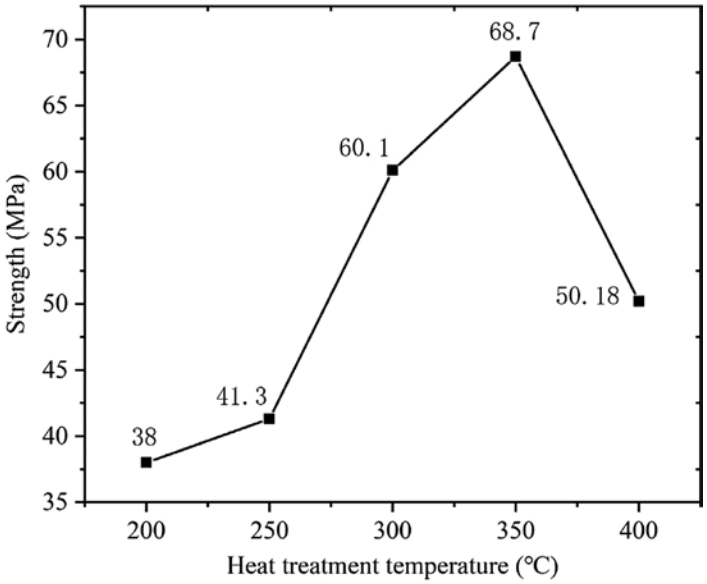

Figure 8: Strength of the Al_2O_3(Ni) ceramic-aluminum alloy joints after 1 hour heat treatment at different temperatures.

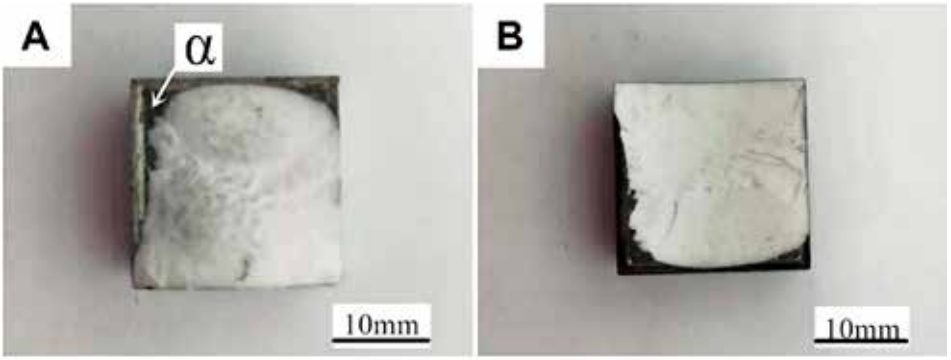

Figure 9: Macromorphology of the 7A52 aluminum alloy-Al_2O_3 ceramic joint fractures after 1 hour heat treatment at 200°C: (A) Fracture on 7A52 aluminum alloy side, (B) Fracture on Al_2O_3 ceramic side.

Location	Al	O	Mg	Si	Ni	P	Phase
1	32.43	65.45	0.92	1.04	0.15	0	Al_2O_3
2	82.3	0.3	2.1	15.3	0	0	Al-Si-Mg solder
3	72.18	1.35	2.44	1.01	22.99	0.04	Al_3Ni
4	27.55	55.1	13.78	1.17	0.1	2.3	$MgAl_2O_4$

Table 4: EDS scan results of each point in Figure 10 (at%).

Figure 9 shows the macromorphology of the 7A52 aluminum alloy-Al_2O_3 ceramic joint fractures under the conditions of heat-treatment temperature 200°C, welding temperature 590°C, holding time 1 hour, and pressure 2 MPa. It can be seen from Figure 9A, B that the white substance was Al_2O_3 ceramic, the gray substance was the solder layer. The fracture occurred partly in the ceramic and partly in the solder layer. A layer of white substance was scattered on the surface of the solder layer, and it should be ceramic.

Figure 10 was the micromorphology of the α zone in Figure 9. From the fracture morphology, it can be concluded the fracture was brittle fracture. Table 4 shows the EDS scan results of four points in Figures 10, 11 showed the XRD diffraction result of the fracture in Figure 10. At position 1, the main composition was Al_2O_3, which was consistent with the previous analysis that the α area was a solder zone but was scattered with ceramic. At position 2, the main composition was Al-Si-Mg solder. At position 3, the main composition was Al_3Ni intermetallic compound. The Al element in the filling material reacted with Ni, which continuously dissolved the nickel-plated layer. And then under the action of pressure, the nickel-plated layer partly broke and scattered in the liquid solder. Position 4 was near position 1, and its main composition was spinel ($MgAl_2O_4$), which meant the active element Mg in the brazing filler metal diffused to the surface of Al_2O_3 ceramic, where it gathered and reacted with the ceramic to form spinel.

CONCLUSION

1. Vacuum heat treatment was carried out for nickel-plated Al_2O_3 ceramics. When the heat treatment temperature was below 300°C, there were few cellular bumps on the surface of the nickel-plated layer, but when above 300°C, there were many cellular bumps on the surface of the nickel-plated layer. According to the results of XRD diffraction analysis, when heat treatment was performed at 350°C and below, the nickel-plated metal had an amorphous structure, and

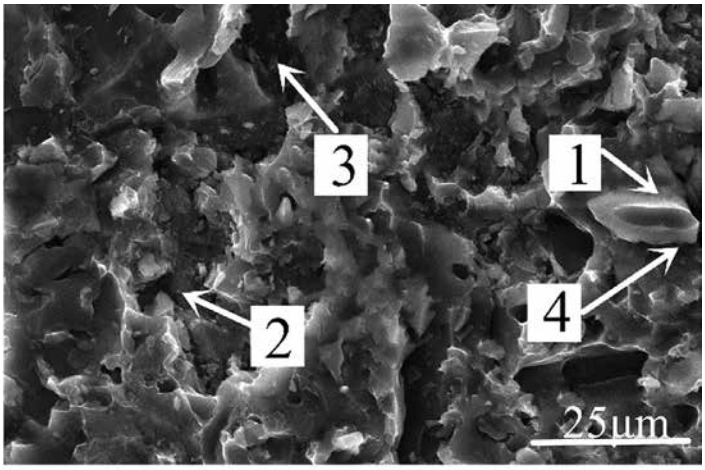

Figure 10: Micromorphology of α zone in Figure 9.

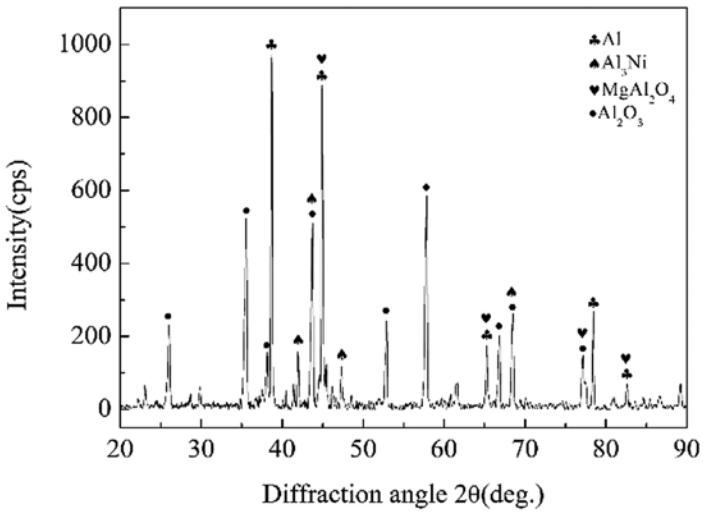

Figure 11: XRD diffraction result of the fracture in Figure 10.

when performed at 400°C, the nickel-plated layer had a crystalline structure, and the brittle phase Ni_3P was precipitated.

2. From Al_2O_3 ceramic to aluminum alloy, the following zones existed at the joint interface: Zr-ceramic reaction zone, brazing filler metal zone, Al-Ni intermetallic compound zone, and Al-Si eutectic zone. Besides, the brazing filler metal zone, Al-Ni intermetallic compound zone, and Al-Si eutectic zone were intertwined. The interface structures of the joint were: Al_2O_3 ceramic/ZrO_2 (minor amount)/spinel ($MgAl_2O_4$)/Al-Si-Mg solder zone/Al_3Ni/7A52 aluminum alloy.

3. Pressure brazing of 7A52 aluminum alloy-Al_2O_3(Ni) ceramic was carried out by Al-Si-MG brazing filler metal. It was found that the temperature of vacuum heat treatment was an important factor affecting the mechanical properties of the joint. The pressure brazing was carried out under the conditions of welding temperature 590°C, holding time 1 hour, pressure 2 MPa. When the heat-treatment temperature was 350°C and below, the joint strength increased with the increase of the heat-treatment temperature. When the temperature was 350°C, the joint shear strength reached the maximum, which was 68.7 MPa, but as the heat-treatment temperature increased to 400°C, the joint strength decreased by 27%-50.18 MPa.

DATA AVAILABILITY STATEMENT

The original contributions presented in the study are included in the article/supplementary material. Further inquiries can be directed to the corresponding author.

AUTHOR CONTRIBUTIONS

DZ: conceptualization and funding acquisition. XQ: methodology, visualization, formal analysis, and writing-original draft. XL: writing-review and editing. KW: resources, validation, project administration and supervision.

FUNDING

This work is supported by the China Postdoctoral Science Foundation (2020M682928) and the Stable Supporting Fund of Science and Technology (WDZC2020JJ021).

CONFLICT OF INTEREST

The authors declare that the research was conducted in the absence of any commercial or financial relationships that could be construed as a potential conflict of interest.

REFERENCES

[1] Ahmad Fauzi, M. N., Uday, M. B., Zuhailawati, H., and Ismail, A. B. (2010). Microstructure and mechanical properties of alumina-6061 aluminum alloy joined by friction welding. Mater. Des. 31, 670–676. doi:10.1016/j.matdes.2009.08.019.

[2] Feng, Y., Chen, J., Qiang, W., and Wang, K. (2016). Microstructure and mechanical properties of aluminium alloy 7A52 thick plates welded by robotic double-sided coaxial GTAW process. Mater. Sci. Eng. A. 673, 8–15. doi:10.1016/j.msea.2016.07.011.

[3] Gama, B. A., Bogetti, T. A., Fink, B. K., Yu, C.-J., Claar, T. D., Eifert, H. H., et al. (2001). Aluminum foam integral armor: a new dimension in armor design. Compos. Struct. 52 (3), 381–395. doi:10.1016/S0263-8223(01)00029-0.

[4] Li, T.-J., Li, G.-Q., and Wang, Y.-B. (2015). Residual stress tests of welded Q690 high-strength steel box- and H-sections. J. Constructional Steel Res. 115, 283–289. doi:10.1016/j.jcsr.2015.08.040.

[5] Nicholas, M. G., and Crispin, R. M. (1982). Diffusion bonding stainless steel to alumina using aluminium interlayers. J. Mater. Sci. 17, 3347–3360. doi:10.1007/BF01203505.

[6] Peng, R., Zhou, H., Ning, X.-S., Xu, W., and Lin, Y.-B. (2002). Research of performance of Al/Al2O3 substrate. J. Inorg. Mater. 17 (4), 731–736. doi:10.3321/j.issn:1000-324X.2002.04.015.

[7] Serjouei, A., Goura, G., Zhang, X., Idapalapati, S., and Tan, G. E. B. (2017). On improving ballistic limit of bi-layer ceramic-metal armor. Int. J. Impact Eng. 105, 54–67. doi:10.1016/j.ijimpeng.2016.09.015.

[8] Song, S., Wang, Y., Jiang, L., Zheng, Y., Chen, Y., and Chen, T. (2020). Progress in electroless plating preparation and applications of Nickel-based amorphous alloys. Mater. Sci. Technol. 28 (1), 81–90. doi:10.11951/j.issn.1005-0299.20180237.

[9] Tasdemirci, A., Tunusoglu, G., and Güden, M. 2012). The effect of the interlayer on the ballistic performance of ceramic/composite armors: experimental and numerical study. Int. J. Impact Eng. 44, 1–9. doi:10.1016/j.ijimpeng.2011.12.005.

[10] Zhang, J.-X., Guan, X.-J., and Sun, S. (2004). A modified Monte Carlo method in grain growth simulation. Acta Metallurgica Sinica 40 (5), 457–461. doi:10.3321/j.issn:0412-1961.2004.05.003.

[11] Zou, G., Aiping, W., Zhang, D., Meng, F., Bal, H., Zhang, Y., et al. (2004). Joint strengthwith soldering of Al203 ceramic after Ni-P chemical plating. Tsinghua Sci. Technol. 9 (5), 607–611. CNKI:SUN:QHDY.0.2004-05-00K.

ABOUT THE AUTHORS

Deku Zhang, Xusheng Qian, Xiaopeng Li, and Kehong Wang are with the College of Materials Science and Technology, Nanjing University of Science and Technology, Nanjing, China. It has been edited to conform to the style of *Thermal Processing* magazine.

THE IMPACT OF COMPLETE LUBRICANT REMOVAL

ON THE MECHANICAL PROPERTIES AND PRODUCTION OF PM COMPONENTS

By comparing the Vulcan process to a conventional sintering process for an EBS lubricant system, it was found the Vulcan process better removed the lubricant while improving physical properties.

By SCOT E. COBLE, JACOB P. FELDBAUER, AMBER TIMS, CRAIG STRINGER, and STEPHEN L. FELDBAUER

The greatest hurdle in the production of powder metal components is lubricant removal. Over the years, equipment and processes have been developed to aid in the removal of the lubricant during the sintering process. Unfortunately, these technologies were not successful in removing all the lubricant.

Recent developments in the sintering process have resulted in a paradigm shift of the way lubricant removal is addressed. This new technology is called the Vulcan process. A process and accompanying equipment, the Vulcan has demonstrated the ability to remove all the lubricant from the compact, the result of which is the increase of physical properties of the sintered part. Transverse rupture strengths can be increased up to 18.0%. Hardness can be increased up to 6.3%. Density can be increased by up to 1.7%. The performance of the Vulcan is also demonstrating a significant opportunity to reduce the cost of production without compromising quality.

INTRODUCTION

Lubricant is needed for the compact to be ejected from the compaction press. The industry has worked to reduce the amount of lubricant that is used, but some lubricant is always needed. The problem occurs during sintering. The particles need to be in contact with one another or physical properties of the component will be detrimentally affected. The once-needed lubricant and oxide from the manufacturing of the powder act as barriers between the particles. Therefore, sintering steps need to remove these barriers to improve the physical properties of the component.

The steps begin with the heating of the compact. This allows the lubricant to melt and be wicked from the part through capillary action. If the lubricant is not removed from the compact, a carbon residue will form and affect the final properties of the product. Next, the atmosphere needs to be manipulated to react with the oxide. Hydrogen (H) is injected to react with the oxide (O^{-2}) forming water H_2O, removing the barrier from the particles. The clean particles of powder are in contact with one another, allowing for a better sinter, resulting in increases in physical properties of the component.

The workhorse of lubricants used in the industry is Acrawax C™. This is an N,N' ethylene bis-stearamide-based synthetic wax (EBS) with a melting point between 284°F to 293°F (140°C to 145°C) [4]. In work done by Powell, Stringer, and Feldbauer, it was shown the optimal lubricant removal temperature for EBS is between 350°F to 1,000°F (177°C to 537°C) [5]. This temperature range is relatively low when compared to sintering temperatures. Temperature control at this low temperature requires convective heating to maintain the low temperature.

Also, in work by Powell, et. al., it was shown if lubricant is exposed to temperatures above 537°C (1,000°F), soot is formed [5]. This sooting causes carbon deposits internally and externally of the part. This carbon contamination in the part causes variations in properties and contamination within the furnace itself.

Until recently, it was thought lubricant exited the compact early in the process, and a "rule of thumb" was 20 minutes for an iron-based compact. In work by Powell, et. al., it was demonstrated weight loss stopped in approximately 22 minutes for parts of 6.2 g/cm^3 density [5]. However, compaction technologies have made significant improvements since then. The typical density of an iron-based product today is above 6.8 g/cm^3, and it is now common for producers to have densities as high as 7.5 g/cm^3 for some products. Also, until recently, it was thought that, with increased density, lubricant removal temperature needed to increase, the opposite of what was described earlier.

In the paper by Powell, et. al., the time to remove EBS as a function of green density was measured, and a mathematical model was developed [5]. The model shows that, with increases in green density, lubricant removal times increase exponentially. Also, as part geometry grows, the pathway for the lubricant to exit the part increases. This requires the component to be in the optimal lubricant-removal-temperature range longer. So, the results of bigger/higher density parts containing EBS are significantly longer lubricant removal times.

In work done by Levanduski and Feldbauer [2] and verified by work done by Powell, et. al. [5], it was shown the hydrocarbon EBS unravels as the temperature increases in the optimal lubricant removal temperature range. The work shows that, as temperature increases, EBS unravels until the simplest hydrocarbon, methane, is formed. The carbon-to-hydrogen ratio of methane is 1:4. EBS has the chemical formula of $C_{38}H_{76}$. Therefore, the carbon-to-hydrogen ratio of EBS is 1:2. Hence, the breakdown of EBS drops carbon. For this reason, Feldbauer describes the need for a very controlled amount of oxygen to react with the carbon. Moisture is the most controllable form of oxidizing media [7]. The H_2O reacts with the dropped carbon, forming hydrogen H_2 and carbon monoxide CO, burning off in the sintering atmosphere. The H_2O flow rate needs to increase with increased lubricant content and production rates as more carbon will be dropped. However, this is a delicate process and accurate control is critical [7]. If too much H_2O injected, then oxidation is the result; if not enough H_2O is injected, then carbon will be left behind.

AN INNOVATIVE APPROACH

Recently, the development of a new technology is resulting in a paradigm shift of how lubricant removal is being addressed. This new technology is the Vulcan process. It gets its name from the Roman god of steelmaking and uses all the knowledge from the research described above. The Vulcan and its accompanying equipment show it can remove all the lubricant from the compact.

The Vulcan uses lower lubricant removal temperatures to prevent

sooting. The optimal temperature range for the removal of lubricants is low in comparison to typical sintering processes. A conventional sintering furnace will have difficulty holding the compacts in this range because of the radiant style of heating used. The result is a rapid heating of the product and lubricant that dissociates to form soot, both internal and external to the compact. This optimal temperature range requires a convective heating source for the initial portion of the Vulcan process. The convective heat transfer coefficient is a strong function of atmosphere chemistry and velocity [1]. This, along with loading and belt speed, provide a great deal of heating control, which enables the time in the optimal temperature range to be adjusted to accommodate the density, product loading, and mass of the compacts.

The Vulcan allows for the manipulation of the atmosphere to rid the particles of barriers. It uses an independent moisture source that provides fine control of the amount of water introduced. The injection location and fine-moisture control provide moisture to react with any carbon dropped during the lubricant break-down. Moisture injection in conventional systems is typically insufficient, difficult to control, or influences the thermal control of the system — all negatively influencing the quality of the lubricant-removal process.

COMPARING PERFORMANCE

To compare the conventional sintering technology to the Vulcan process, FC-0208 powder was paired with the lubricant Acrawax C TM (EBS). Lubricant content of the samples varied from 0.30 wt%, 0.50 wt%, and 0.75 wt%. Density of the samples varied from 6.8 g/cm^3, 7.0 g/cm^3, and 7.2 g/cm^3. The Transverse Rupture Strength (TRS) bars were loaded in two conditions (Figure 1). They were loaded in either Single Stack or Double Stack loading. In Single Stack loading, TRS samples were placed on top of ceramic plates. In Double Stack loading, TRS samples were placed in between ceramic plates; this loading was done to simulate the doubling of production. These loadings were used as worst-case scenarios as they increase thermal mass and hinder interaction with furnace atmosphere. The samples were then sintered either with the conventional process or with the Vulcan process.

The conventional and Vulcan furnaces each contain eight zones of heating control, four zones in the high-heat section, and four zones in the pre-heat section. Both furnaces have a 240 inch (6.10 m) pre-heat box; both have a 240 inch (6.10 m) high-heat section. The cooling sections in the Vulcan and conventional furnaces are identical. The only difference, in appearance, is that the Vulcan has a 4 foot (1.22 m) Zone 0 that allows the compact to be exposed to hot gases moving forward in the furnace before parts enter the pre-heat box. These zones were set for each furnace to achieve optimal lubricant removal. Both processes were set with the belt speed of 6 in/min (15.2 cm/min), sintering temperature of 2,075 °F (1,135°C), and approximately 22 minutes at the sintering temperature for each system. Note sintering times are the time that the compact is within 50°F (28°C) of the target sintering temperature.

The thermal profiles of the two processes reveal where the paradigm shift lies. The difference allows the part to be in the optimal lubricant temperature range, 350°F to 1,000°F (177°C to 537°C), 2.4 times greater in the Vulcan furnace compared to the conventional furnace.

WEIGHT LOSS

Weight loss was evaluated from green to sintered. All weight losses were greater than the original amount of lubricant. Recall there are two factors that contribute to weight loss: the removal of the lubricant and the removal of oxygen during the oxide reduction step.

Figure 1: Photo of TRS bars entering conventional furnace. Single-layer loading on the right, double-stack loading on the left.

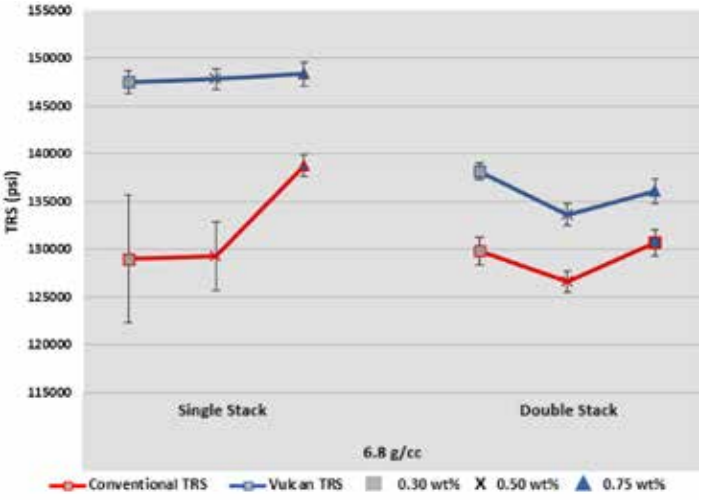

Figure 2: Transverse Rupture Strength (psi) for 6.8 g/cm^3 density vs. lubricant content.

However, this type of comparison is still relevant as the amount of oxide in the powder is assumed to be equal, so any difference in weight loss can be attributed to the loss of lubricant.

In all cases, the weight loss was less in the conventional process for all comparable conditions. However, the differences were very small. It is also important to note that weight loss is often better for the Vulcan double stack condition when compared to conventional single stack of comparable conditions.

This difference can be explained by a couple of contributing factors. First, the TRS bars being on the ceramic plates increase thermal mass and slows the heating rate of the samples. With the belt speeds being identical, this causes the time the samples are in the optimal lubricant temperature range to be slightly less in the double stack condition. Second, the loading condition hinders interaction with furnace atmosphere. This hindrance with the sintering atmosphere would slow the reaction with the exiting lubricant. This slowing of the reaction can lessen weight loss by leaving some lubricant/

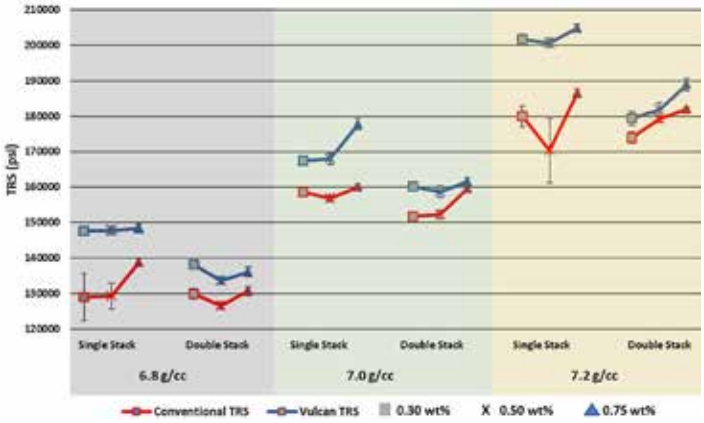

Figure 3: Combined TRS strengths vs. lubricant content.

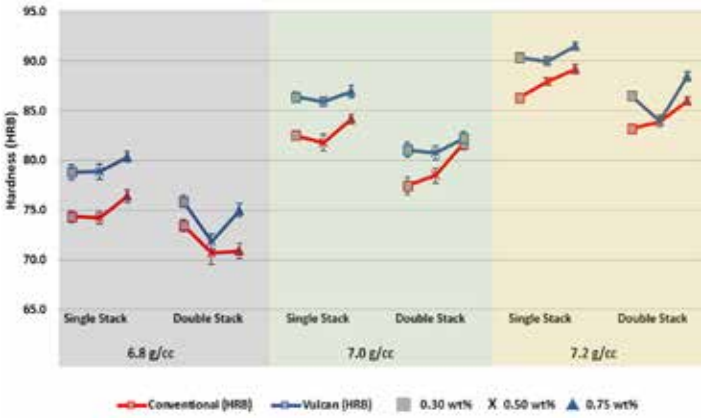

Figure 4: Combined Hardness Rockwell B (HRB), with error bars, vs. lubricant content.

carbon behind.

The weight loss study data showed some differences, but the data was inconclusive on which process was performing better.

TRANSVERSE RUPTURE STRENGTH (TRS)

Transverse Rupture Strength data was collected from each processing condition. The thought was that, with more lubricant removed from the compact, the particles would be in greater contact with one another. This would result in a better-quality sinter and increases in Transverse Rupture Strengths. The data shows that TRS strengths are greater for the Vulcan in all comparable conditions.

Figure 2 is the TRS strength data for the molded density 6.8 g/cm^3. The red lines are the conventional data, and the blue lines are the Vulcan data. The lubricant content increases to the right, with the square 0.30 wt%, X 0.50 wt%, and triangle 0.75 wt%. The single stack loading data is grouped on the left and double stacked on the right. The TRS strengths favor the Vulcan by 6.9 to 14.4%. The samples processed in the Single Layer condition in the Vulcan have TRS strengths that vary by less than 0.6%. This shows that, at this molded density and condition, the Vulcan provides little variability in TRS strengths, no matter lubricant content.

The data from Figure 3 continues to demonstrate the importance of the lubricant removal. As the molded density is increased, there is a significant improvement in strength for those samples sintered in the Vulcan process.

At a molded density of 7.2 g/cm^3, a density that is known to be a challenge for the EBS system, the Vulcan shows a large improvement in the properties of the product. This density yields differences in TRS strengths up to 18.0% greater for samples sintered in the Single Layer condition and 3.8% for samples sintered in the Double Stack condition.

Overall, the Vulcan's TRS strengths are greater for the Single Layer condition by 5.6 to 18.0% and for the Double Stack condition by 1.2 to 6.4%. Therefore, the Vulcan produces better quality parts no matter the lubricant content or density.

In nearly all cases, the product sintered in a double-stacked condition on the Vulcan has strengths equal to or better than those sintered in a single-stacked condition on the conventional system. In the double-stacked condition, the Vulcan has strengths up to 7.1% better than those sintered in a single stacked condition on the conventional system. This would indicate the Vulcan has the potential to produce at twice the production rate and still produce a product equal to or superior to one sintered on a conventional furnace.

HARDNESS: ROCKWELL B (HRB)

During the processing of the TRS samples, parts were allowed to normalize. Therefore, any difference seen in hardness can be attributed to lubricant removal increasing the quality of sinter, not from processing. With the lubricant removed, there is no barrier between the particles. With the particles in greater contact with one another, porosity is decreased. The result of decreasing porosity is increasing hardness. The data shows hardness values favor the Vulcan Process for all comparable conditions. The Vulcan increases hardness in the Single Stack condition from 2.4% to 6.3% and in the Double Stack condition up to 5.8%.

Data from Figure 4 shows the largest difference in hardness is seen in the 6.8 g/cm^3, 0.50 wt% single layer samples. The HRB hardness favors the Vulcan process by a difference of 6.3%. This can be explained by lubricant removal increasing the quality of the sinter. The 6.8 g/cm^3 samples are the most porous of those tested. The more porosity the lower the hardness value. Therefore, a better-quality sinter in a porous sample, results in a larger percent difference in hardness.

As molded density increases, the samples become less porous. The result of less porosity is an increase in hardness. The data shows the importance of lubricant removal. The Vulcan provides an increase in hardness for all comparable conditions. In the 7.0 g/cm^3 samples, the Vulcan increases hardness by 3.2% to 5.1% in the single layer condition and 0.7% to 4.6% in the double stack condition. The Vulcan 7.2 g/cm^3 density single stacks samples hardness values are increased by up to 4.7% and by up to 4.0% in the double stack condition.

The data in Figure 4 reveals Vulcan hardness values are greater for all comparable conditions no matter the lubricant content or density. Therefore, the hardness data shows that, by removing more lubricant, the Vulcan provides a better-quality sinter compared to the conventional furnace.

DENSITY

The removal of all the lubricant will allow for a better-quality sinter because the particles will be in greater contact. This greater contact will reduce porosity within the component and, therefore, increase density.

The 6.8 g/cm^3 density samples from both processes were evaluated for Archimedes density. The data shows the Vulcan provides more dense parts. In the single-layer condition, the Vulcan increases density by 1.2% and in the double stack condition by 1.7%.

The greater increase in the double-stack condition can be explained by the fact that the conventional furnace struggles with lubricant removal in this loading condition. In nearly all the testing, in all comparable conditions, the conventional double stack saw the

lower values. This being lower allows for a greater increase in physical properties.

SCANNING ELECTRON MICROSCOPE (SEM) IMAGES AND PORE ANALYSIS

The Vulcan is providing an increase in all the properties tested. With all the lubricant removed, the particles would be in greater contact. This contact is providing a better-quality sinter.

Figure 5 shows the fracture surfaces of 6.8 g/cm^3, 0.50 wt% samples with the conventional sintered sample on the left and the Vulcan process sample on the right. Both scanning electron microscope (SEM) images are at 160X. Note the fracture surface of the sample sintered in the Vulcan is less porous and appears to have more of a shear fracture surface, compared to the more porous facture surface of the conventional sample. Therefore, the Vulcan, by appearance, is providing a better-quality sinter.

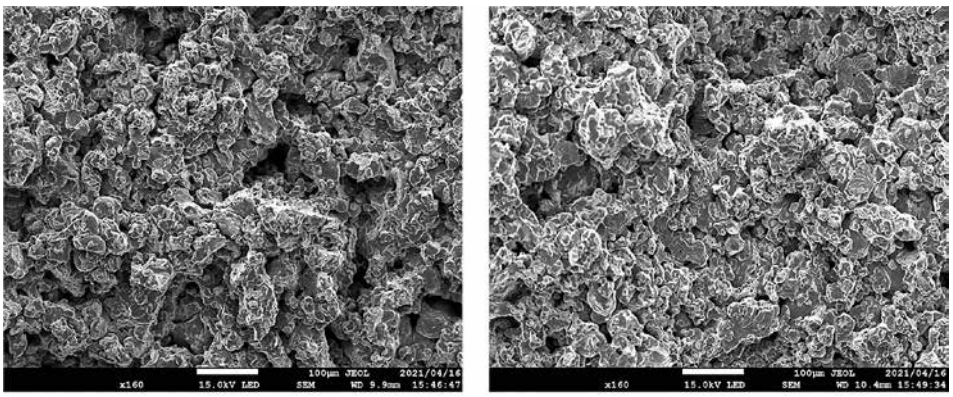

Figure 5: Sintered scanning electron microscope (SEM) images at 160X. Conventional on left, Vulcan on right. Samples are both of 6.8 g/cm^3 density and 0.50 wt% lubricant content.

Also, with more lubricant removed, there would be less carbon present within the pores of the compact. FC-0208 powder has a nominal carbon content of 0.6 wt% to 0.9 wt% [3]. Using the SEM, the pores of the fractured 6.8 g/cm^3, 0.50 wt% samples were evaluated for what elements were present. The analysis revealed the average pore carbon present in the conventional sample is 10.4 At%. While the Vulcan's average pore carbon content is 6.4 At%. Therefore, the conventional process leaves 64% more carbon behind in the pores than the Vulcan process does. This difference in carbon content results in TRS strengths increased by 14.4%, hardness improvement of 6.3%, and a 1.2% denser part.

TOTAL CARBON

Total carbon analysis was conducted on the same 6.8 g/cm^3, 0.50 wt% samples. This was done to further verify the Vulcan process is removing more lubricant than the conventional process. With the amount of carbon within the powder being consistent, any difference seen in the total amount of carbon can be attributed to lubricant not removed. Therefore, the lesser the amount of carbon present, the more lubricant was removed.

The data shows there is less total carbon in the parts processed in the Vulcan no matter the condition. In the single-layer condition, the Vulcan total carbon was found to be 0.73% compared to the conventional 0.74%. With less carbon in the part, physical properties are increased: TRS strength by 14.4%, hardness by 6.3%, and density by 1.2%.

Likewise, in the double-stack condition, the Vulcan total carbon of 0.73% betters the conventional 0.74%. The lesser amount of carbon in the part increases physical properties: TRS strength by 5.6%, hardness by 4.3%, and density by 1.7%.

CONCLUSION

A comparison was made of the Vulcan process to a conventional sintering process for an EBS lubricant system at various lubricant contents, densities, and loading conditions. In all cases, the Vulcan demonstrated the importance of removing the lubricant and the resultant improvement on physical properties.

Complete removal of the lubricant greatly improves the properties of a sintered component. A part loaded in a single layer on the Vulcan may have up to an 18.0% better Transverse Rupture Strength, up to 6.3% better Rockwell B hardness, and 1.2% increase in density than one sintered in a single layer on a conventional furnace.

The data shows there is less total carbon in the parts processed in the Vulcan no matter the condition.

The Vulcan affords two distinct advantages over the conventional sintering process. The producer has a choice in how to realize these advantages. They can produce a superior quality product, or they can produce a comparable quality product at twice the rate.

SPECIAL THANKS

The authors would like to extend a special thanks to Symmco Inc. for granting us access to its laboratory. Without Symmco's cooperation and hospitality, the project would not have been possible.

REFERENCES

[1] DeWitt, F. P. (2002). Fundamentals of Heat and Mass Transfer. New York: John Wiley & Sons, Inc.

[2] Edward Levanduski and Stephen L. Feldbauer, P. (2010). Observations in Lubricant Removal. PowderMet (pp. Presentation, Special Interest Session). Fort Lauderdale, FL: Metal Powder Industry Federation.

[3] Federation, Metal Powder Industries. (2007, April 16). Material Standards for PM Structural Parts. Princeton, NJ: Metal Powder Industries Federation. Retrieved from MPIF Standard 35.

[4] Lonza Group. (2011, February 9). Lonza_ProductDataSheets_Acrowax_PDS_29679(3).pdf. Retrieved from http://bio.lonza.com/go/literature/2805.pdf.

[5] Robert Powell, C. S. (2013). Lubricant Transport within a Powder Metal Compact durnign Pre-Sinter. PowderMet. Chicago, IL: Metal Powder Industry Federation.

[6] Standard Test Methods for Metal Powders and Powder Metallurgy Products. (2010). Princeton, NJ: Metal Powder Industry Federation.

[7] Stephen L. Feldbauer, P. (2020, January). A Review of Lubricant Removal Systems and the Latest Technology. Industrial Heating, pp. 24-27.

ABOUT THE AUTHORS

Scot E. Coble and Jacob P. Feldbauer are with The Pennsylvania State University. Amber Tims, PMT, is with the North American Hoganas Co. Craig Stringer, Ph.D., is with Atlas Pressed Metals. Stephen L. Feldbauer, Ph.D. is with Abbott Furnace Company.


YOU'VE GOT THE PRODUCTS.
YOU'VE GOT THE SERVICES.
NOW, LET US SHARE YOUR STORY.
Thermal Processing wants to make sure the best possible audience knows your company. Through our print, online, and social media presence, our experienced staff can get your message to an industry that wants to know what you can do.
Thermal processing
To learn more, contact national sales director Dave Gomez at dave@thermalprocessing.com or call 800.366.2185 ext. 207

COMPANY PROFILE ///

BUEHLER

INNOVATIVE SOLUTIONS AND EXPERT SERVICE

Buehler has a lab team full of material-science professionals who are constantly working to develop new processes to prepare materials for the heat-treat industry. (Courtesy: Buehler)

Buehler is a manufacturer of metallographic testing equipment including scientific instruments and supplies for cross-sectional material testing.

By KENNETH CARTER, Thermal Processing editor

For 85 years, Buehler has been at the forefront in the field of materials analysis, offering state-of-the art materials preparation and analysis equipment, as well as innovative software solutions.

It's a credit to the company's Swiss roots that allow it to continue to be a major player for a variety of industries, including heat treating.

"We are a provider of full lab solutions for materials analysis and preparation," said Sarah Beranek, Americas commercial director for Buehler. "We design, manufacture, and distribute products in sectioning mounting, grinding and polishing, hardness testing, and imaging analysis. The equipment, as well as the consumables and supplies for that equipment, is based around the 80 years of material-science knowledge we have in house. We really strive to elevate and retain that technical knowledge in the company. We have a lab team full of material-science professionals who are constantly working to develop new processes to prepare materials for the heat-treat industry — that being a very large segment of ours. That feeds into, of course, a lot of broader market segments like automotive and aerospace."

FULL LAB SOLUTIONS

All that development surrounds Buehler's mission statement to offer full lab solutions and products for materials preparation analysis, according to Beranek.

"In the world of heat treat, it's really appreciating and understanding those specific needs of high-volume applications of production, oftentimes around automation, reliability, and repeatability," she said. "How do you build both preparation and analysis processes that enable high volume usage? We do that by offering advanced software solutions to minimize user interaction during those analysis steps and build out a robust capability to follow industry standards from ISO to ASTM. Buehler adheres to ISO 9001, 14001, and 17025 practices, and we appreciate that our customers in the heat-treat industry follow some pretty rigorous internal standards for quality tracking and traceability. So, we try to build solutions in our products to really support those needs."

INNOVATIVE SOFTWARE

A big part of the Buehler's capabilities stems from its software solutions designed to make processes such as hardness testing both easier and quicker, according to Beranek.

"In the world of automation, one of our hardness testing products we're very proud of is our DiaMet software solution," she said. "Traditionally, when you go to do hardness testing for case hardening, you'd need to manually develop an indent path across the case hardening zone."

Buehler's DiaMet software solutions are capable of performing that mapping across the entire part, according to Beranek.

"For example, you can build out a single job or program that enables you to map out an indent pattern automatically over a whole area of interest like a gear tooth," she said. "And then that translates into a heat map of hardness values. That has been a big focus area in our hardness testing automation spaces. How do you build out those automated solutions to meet those high-volume needs? And then while doing it, how do you make sure you have all of your test block calibrations throughout your shifts recorded and ready for your ASTM audits or your ISO audits?"

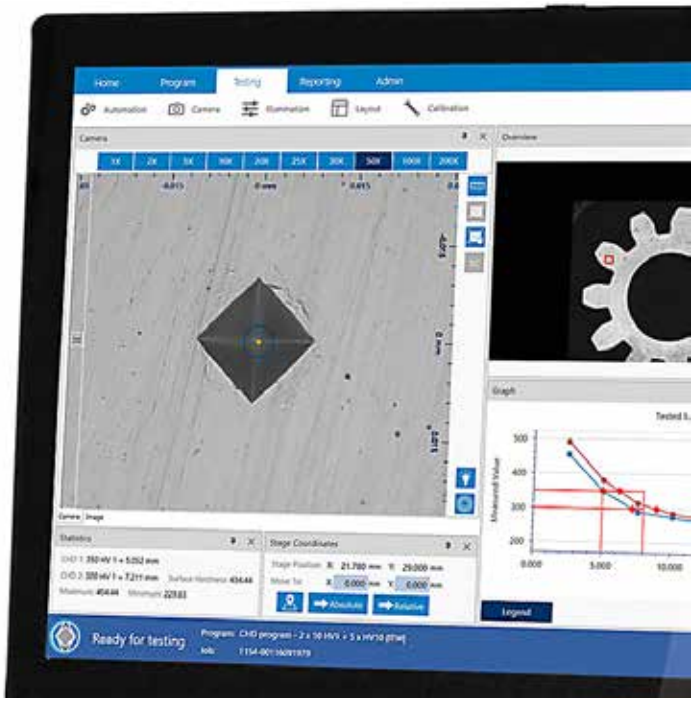

Buehler's DiaMet software can map across the entire part. (Courtesy: Buehler)

ADDRESSING CUSTOMER NEEDS

That type of innovation is important, especially when customers' challenges can often run the gamut of difficulty levels.

"When a customer approaches us with a particular pain point or challenge, we can rely heavily on our entire sales and support staff that have in-depth knowledge of the applications in which our customers are using our products," Beranek said. "We really make sure we nail down the real pain point of what our customers are trying to solve — what it is very specifically that's giving them a challenge."

After that initial analysis, Beranek said Buehler's experts come back with a multifaceted approach: Does the solution lie in a different process or piece of equipment? Do you just need a different software solution or a customization to existing software? Is it actually something further back in your process that's causing the problem?

"A lot of times, hardness testing and imaging analysis results can

be skewed dramatically by the preparation route you use to get there," she said. "We find that often the root cause of a pain point isn't necessarily what was expected at the initial interaction. So, we really try to dig in and go through that kind of root-cause methodology with our customers to make sure that we're solving the right problem with them. And again, with our focus on full-lab solutions, we can help solve problems that may stem earlier in their analysis process than they realize."

85-YEAR HISTORY

The Swiss roots mentioned earlier come from the company's founder: Adolph Buehler, a Swiss immigrant who started the company in Chicago in 1936. He saw the underserved need for materials preparation and analysis and started taking research-oriented products and transforming them into more production-type products to support the industry.

The hardness-testing side of the company came through its 2011 acquisition of Wilson, a company whose claim to fame includes the development and production of the world's first Rockwell hardness tester.

Through those 85 years, Buehler has been an industry leader in many areas, but Beranek pointed out that the company's recent history in dealing with the COVID pandemic has been a particular source of pride.

"I think Buehler as a company, our employees, and our customers have shown a ton of resiliency in getting through the unprecedented circumstances caused by the pandemic," she said. "We have been very proud of our ability to service essential businesses uninterrupted throughout the health crisis. We provide testing equipment and supplies into a wide variety of medical and infrastructure applications worldwide. This continuity of service and support was the result of being creative in meeting customer needs remotely and being proactive to ensure a smooth supply chain of testing supplies to essential businesses."

Buehler adheres to ISO 9001, 14001, and 17025 practices. (Courtesy: Buehler)

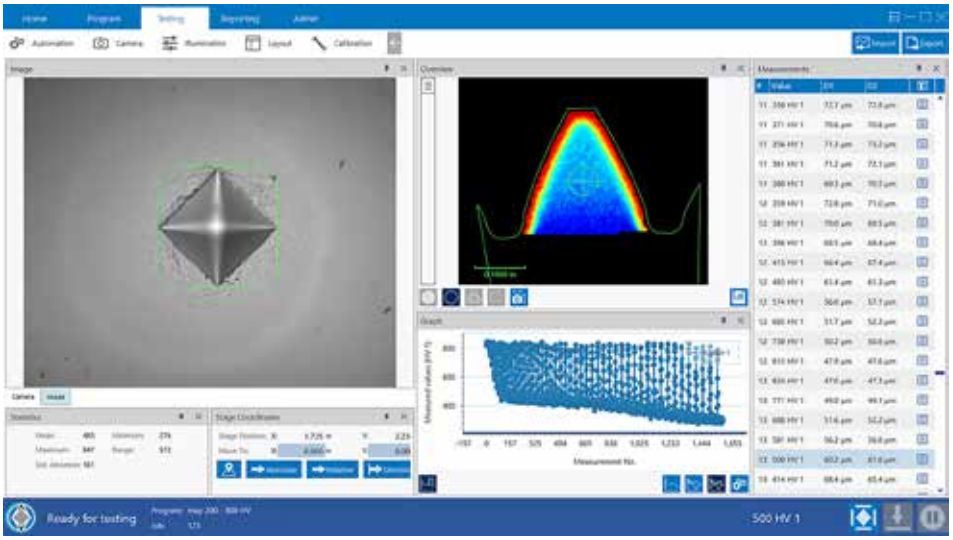

A big part of Buehler's capabilities stems from its DiaMet software, designed to make processes such as hardness testing both easier and quicker. (Courtesy: Buehler)

ENVIRONMENTAL INITIATIVES

Not only has Buehler been a critical source of the pandemic network, but Beranek also pointed out the company has made many strides in being more environmentally friendly.

"We've had a really strong shift toward an environmental focus over the last 10 years," she said. "Today at our Buehler headquarters, we use 100 percent renewable energy sources. We internally use as much reusable packaging as possible such as wooden crates that go back and forth with our own suppliers. We've been able minimize our landfill and recycling weight coming out of our building year over year. This focus translates to our products as well. We appreciate the safety and health needs of our customers. A lot of the supplies and consumables in the world of preparation can pose health hazards, so we're continually developing our supplies to minimize those health hazards. In addition, we prioritize designing new consumables to last as long as possible in order to minimize waste and time to replacement. That's been a big focus for us."

With a focus on the environment and its customers' needs, Beranek said Buehler will continue to invest in new consumables, software solutions, automation, traceability, auditability, and more.

"We certainly see the need for more automation and the ability to manufacture, prepare, and test a higher volume of products in the world as markets grow," she said. "We also see, of course, a shift in markets — vehicle electrification, for example — and some of the traditional primary metals and heat-treat applications are shifting along with it. We see the need to stay on top of what that means for material science in the world, and what kind of quality checks need to be done to ensure a safe and high-quality end product. We strive to ensure we're ahead of the curve and that we're there for our customers when they start to have a new process or material that they need a solution for."

MORE INFO www.buehler.com

MARKETPLACE ///

Manufacturing excellence through quality, integration, materials, maintenance, education, and speed.

Contact **Thermal Processing** at 800-366-2185 to feature your business in the Marketplace.

ADVERTISER INDEX ///

PETER CAINE /// DIRECTOR OF CUSTOM PRODUCTS /// HEATTEK

"We're in a significant growth period at HeatTek and have made a commitment to serve some of the world's most critical industries, many of which have high manufacturing demands."

What is your role with HeatTek and what's a typical week like?
My position at HeatTek is director of Custom Products. Our custom products division handles all of our furnace applications as well as our unique applications that are often focused on certain major markets including automotive, aerospace, the aluminum industry, and the foundry industry. Those four industries get us into many different projects, but a typical day at HeatTek for me revolves around managing our current projects that are in-house with our dedicated team of application and design engineers, and managing new and incoming projects through our applications engineering group. My part of that is filtering what projects we quote helping us focus on the industries in which we want to concentrate. And then from a marketing standpoint, we're involved in our marketing pretty much daily, generating new business leads through our digital partnerships, website, and social media.

What products does HeatTek offer the heat-treat industry?
Within the automotive, aerospace, aluminum, and foundry industries, we offer ovens and furnaces in temperature ranges up to 2,000 degrees Fahrenheit, which is really where we top out. We also get into some atmosphere environments, primarily in nitrogen or hydrogen atmospheres, but the lower-temp furnace applications are what we are best at. Our projects in general can be in the half-million-dollar range and easily over a million-dollar range.

HeatTek recently opened an additional facility in Ixonia, Wisconsin. What role will this facility play in HeatTek's future?
As we grow and increase our yearly revenue, it's going to require more personnel for one thing. We no longer can produce enough out of the single location. Our newest addition, which we're now calling Plant Two in Ixonia, will be primarily for logistics and some manufacturing potentially in the future, but primarily management of incoming and outgoing materials and warehousing—all to optimize our manufacturing efficiency.

HeatTek also recently acquired another plant. What is its purpose and why did HeatTek feel the need to add it?
HeatTek's third plant is located in Milwaukee. We acquired this location solely because of the additional manufacturing space required for the large systems that we build. This is a building twice the size of our current location with multiple phases of manufacturing and is suited very well for the largest machines we build, as well as multiples of those machines being built at one time.

Where do you see the heat-treat industry in the next decade and HeatTek's place in that future?
Our place in the industry today is serving the low-end temperature range of the heat-treating market. With the current logistics issues and shipping challenges, the heat treat industry here in the United States will be as strong as ever, and building those products we need domestically will be increasingly more important. And the integration of automation into that manufacturing is what HeatTek will have a part in. It's going to be a growing market for us at HeatTek because of that.

Anything you'd like to add that we didn't talk about?
We're in a significant growth period at HeatTek and have made a commitment to serve some of the world's most critical industries, many of which have high manufacturing demands. This is part of the reason for our recent expansion. We've also just reached 22 years of being in business, which is a milestone that is worth celebrating as we look back on everything HeatTek has accomplished for our customers during that time.

MORE INFO www.heattek.com

CRYOFURNACE | CRYOTEMPER | CRYOFREEZER

MULTIPLE TEMPERS. ONE CYCLE.

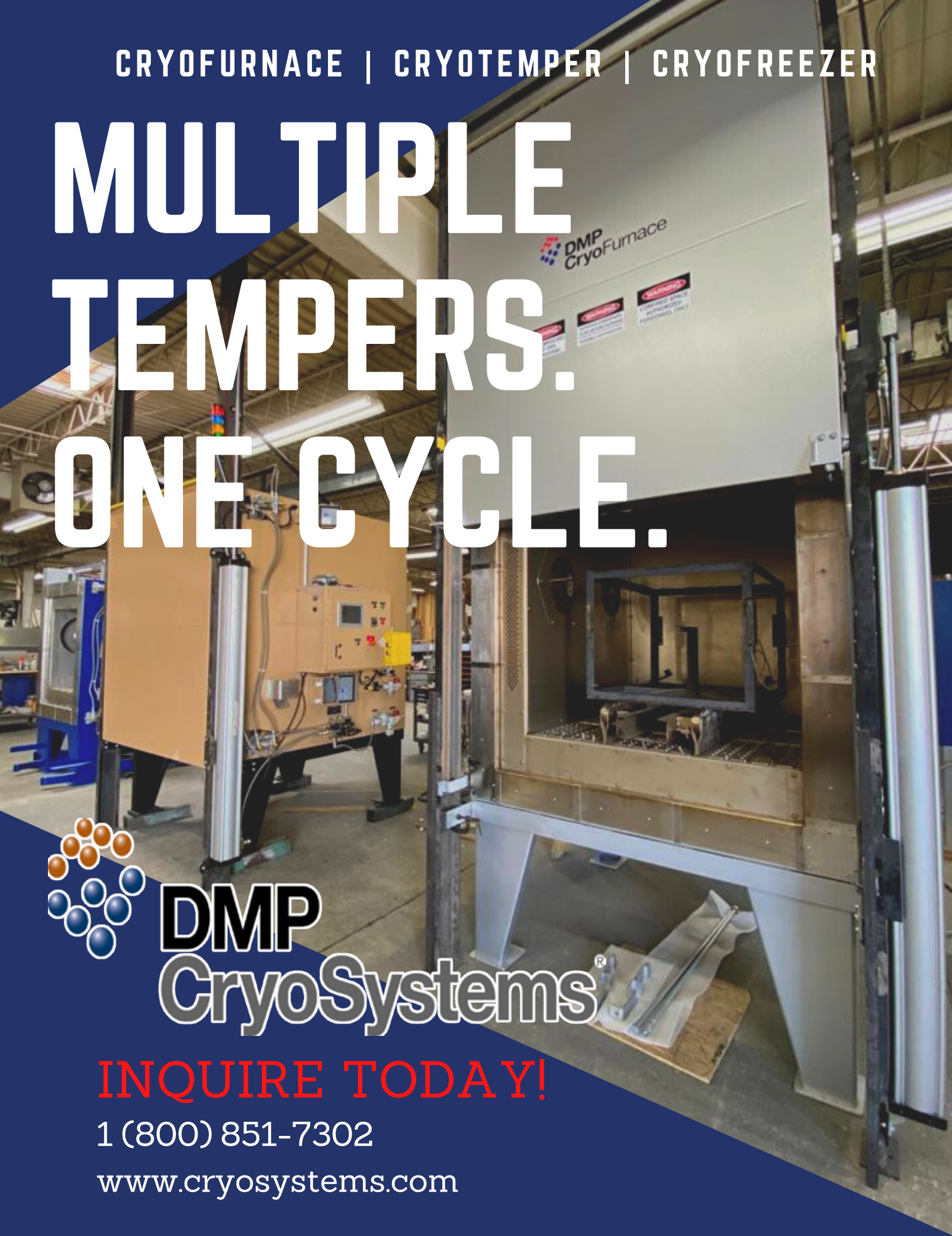

DMP CryoSystems®

INQUIRE TODAY!

1 (800) 851-7302

www.cryosystems.com

VACUUM HEAT TREATING
FURNACES


Compact, internal quench


Production ready, internal quench


Production ready, external quench

Mid-sized, internal quench


Vertical bottom loading


High capacity, car bottom loading

SOLUTIONS THROUGH INGENUITY

Solar Manufacturing designs and manufactures high performance, technically advanced and energy efficient vacuum heat treat furnaces. Models range from compact R&D size furnaces to mid-size horizontal production furnaces to huge car-bottom vacuum furnaces for large heavy workloads. No matter what the application or size of workload, Solar Manufacturing has the versatile, feature-rich vacuum furnace solution to fit your needs. We back it all up with outstanding Aftermarket support: spare parts, service and replacement hot zones.

SOLAR MANUFACTURING

267.384.5040
sales@solarmfg.com

solarmfg.com

Give us a call to learn more about our vacuum furnace ingenuity.